

CONCORDIA UNIVERSITY

RELEASABLE
DOC-CR-RC-81-062



Technical Note No. TN-EMC-81-01
Interim Report No. 2
January 19, 1981

"Resonant Behavior and the Detuning of
Power Lines in the MF Band"


C.W. Trueman and S.J. Kubina
Electromagnetics Laboratory
Concordia University/Loyola Campus

FACULTY OF ENGINEERING

TK
6553
I787
1981
#01
ISSN
#01

IC

1455 de Maisonneuve Blvd., West
MONTREAL, H3G 1M8, Canada

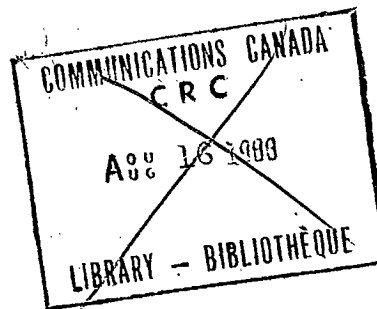


Loyola Campus
7141 Sherbrooke St. W.
Montreal, Quebec
H4B 1R6

Technical Note No. TN-EMC-81-01
Interim Report No. 2
January 19, 1981

"Resonant Behavior and the Detuning of
Power Lines in the MF Band"

C.W. Trueman and S.J. Kubina
Electromagnetics Laboratory
Concordia University/Loyola Campus



Industry Canada
Library - Queen

AOUT 20 2012
AUG

Industrie Canada
Bibliothèque - Queen

APPROVED FOR PUBLIC RELEASE; DISTRIBUTION UNLIMITED

SCIENTIFIC AUTHORITY
G.M. ROYER

Prepared for :

Communications Research Centre
Ottawa, Ontario K1A 0S5
Contract No. OSU80-00121

1950-1951

TK
6553
T 787
1981
#01
5-05

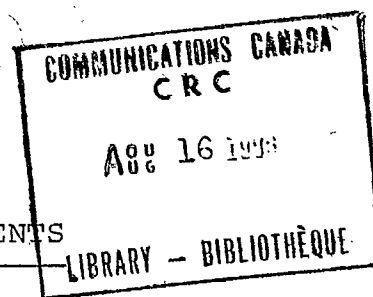


TABLE OF CONTENTS

	Page
TABLE OF CONTENTS.....	i
1. Introduction.....	1
2. Stub Detuning For the Two Wavelength Resonance Mode	2
2.1 Resonance and Detuning.....	2
2.2 Mechanism of Operation and Optimum Design.....	3
2.3 Conclusion.....	4
3. Frequency Dependence From 200 To 1100 kHz.....	4
3.1 Convergence of the Solution.....	4
3.2 Verification Against Measured Results.....	6
3.3 Frequency Dependence.....	6
3.3.1 Max-to-Min Ratio.....	6
3.3.2 The Integrated Current.....	7
3.4 Azimuth Pattern as a Function of Frequency.....	8
3.5 RF Current Distribution and Resonance Modes.....	9
3.6 Resonance Chart.....	10
3.7 Summary.....	11
4. Preliminary Study with Finite Ground Conductivity..	11
4.1 The Monopole and Ground Screen.....	12
4.2 Antenna Plus Power Line.....	12
4.3 Comparison of the RF Current Distributions.....	13
4.4 Summary.....	13
5. Further Work.....	14
5.1 Detuning.....	14
5.2 Finite Conductivity Ground.....	14
REFERENCES.....	15
FIGURES.....	16-38

Resonant Behavior and the Detuning of
Power Lines in the MF Band

by C.W. Trueman
and S.J. Kubina

1. Introduction

Report No. 1 (1) of this project contained a study of the resonant behavior of a nine tower power line model over a wide frequency range, and identified the "one wavelength" and "two wavelength" resonance bands. Also, in that report the modelling of detuning stubs on the skywires was addressed, and the azimuth patterns measured at NRC using three large towers with one and two detuning stubs were reproduced by calculation, and so the validity of the numerical model of the detuning stub was established.

In this report the detuning stub model is exploited to explore the mechanism which makes the stub effective, and to seek an optimum location on the skywire and an optimum length for a detuning stub for the two wavelength resonance region. Also, the frequency dependence of the re-radiation from a five tower power line is investigated in response to Don Jones' request(2). The study identifies a limitation of the computer model in the one wavelength resonance region, and re-examines the postulated current modes of Reference (1). Finally, this report contains an initial investigation of the modelling of the finite conductivity of the ground, which indicates that the azimuth patterns will not be greatly different from those obtained from the model with a perfectly conductive ground.

2. Stub Detuning For the Two Wavelength Resonance Mode

In Reference (1) the validity of the numerical model of the detuning stub of Fig. 2.1 is established in comparison to Lavrench and Dunn's measurements on a three tower power line using 200 scale factor towers. In this chapter the mechanism that makes the stub effective is explained and the optimum length and location for the stub are given. The material forms part of a submission to the IEE Second International Conference on Antennas and Propagation(3).

In Reference (1) Fig. 6.2 compares the azimuth pattern of the three tower power line from the computer model to the measurement, with good agreement. Fig. 2.2 in this report shows the RF current distribution on the towers and skywires of the power line of Fig. 2.1, with no detuning stubs. For each tower, the current is shown at a point one-quarter the height of the tower above ground, and again at three quarters the height. The current is shown on each skywire at ten evenly spaced points. It is seen that for two wavelength loop resonance, the current is a standing wave with constant phase with distance along the skywire. Also, the current has sharp minima near each tower, where the phase changes by 180 degrees.

2.1 Resonance and Detuning

Fig. 2.3 shows how the max-to-min ratio changes as the frequency is swept through the two-wavelength loop resonance region. With no detuning stubs, the power line displays a broad resonance at about 860 kHz in the calculated results and 875 kHz in the measured data, which is from Reference (4). The purpose of adding detuning stubs to the power line is to suppress the RF current and so also suppress this resonance in the frequency dependence. Thus the stub shown by the solid line in Fig. 2.1 was added, with the "separation" "d" chosen as one-twentieth of the wavelength at 860 kHz or 17.4 m, and the "length" "l" chosen as one-quarter wavelength at the same frequency, or 87 m. Fig. 2.3 shows that the max-to-min ratio with the stub is less than one dB across most of the band being considered, indicating that the azimuth pattern is nearly circular. The max-to-min ratio has a minimum value near the "design" frequency of 860 kHz and rises quickly above that frequency.

A second detuning stub was added to the model as shown by the dashed lines in Fig. 2.1, with its "design frequency" chosen as 740 kHz. Fig. 2.3 shows the calculated and measured max-to-min ratio with the two stubs in place. The effect of the second stub is primarily to suppress the rising max-to-min ratio below 750 kHz. The stubs in the computer model are more effective than those in the measurement model. The computed data could be made to reproduce the measurement more closely by

adjusting the dimensions of the computer model to match those of the scale model more precisely, but this was not pursued.

2.2 Mechanism of Operation and Optimum Design

The separation of the stub and end effects at the open wire end contribute additional length to the stub so that the optimum choice is not simply one-quarter of the free space wavelength at the design frequency. Also, as will be shown, the effectiveness of the stub is strongly dependent on where it connects to the skywire. These considerations were investigated using a "power line" of nine towers, with tower height and separation of 166 and 900 feet respectively, excited by an omnidirectional broadcast antenna directly opposite the center tower with separation and height of 1470 and 640 feet respectively. The azimuth pattern of this configuration is similar to that of the three tower power line. In the following a comparison is made between the "straight" stub oriented perpendicular to the skywire, as shown in Fig. 2.4, and the "bent stub" which is parallel to the skywire for most of its length.

The primary effect of including nine towers in the model instead of three is that the minima in the azimuth pattern are much deeper, and so the resonance peak in the max-to-min ratio vs. frequency graph, shown in Fig. 2.5, is much higher than that of Fig. 2.3 for three towers. This resonance is effectively suppressed by either the "straight" or "bent" stub, as shown by the curves of Fig. 2.5. The stub works because it is a low impedance element connected to a high impedance point on a resonant structure, and so destroys the resonance. The stub with its image in ground constitutes a two-wire transmission line one-quarter wavelength long, which is approximately open-circuited at one end. Thus at the point of connection to the skywire-and-image transmission line, the quarter wave stub presents a low impedance. It will now be shown that the point where the stub is connected strongly affects the performance of the stub, and that the best location is a high-impedance point on the resonant power line.

Fig. 2.6 shows the max-to-min ratio at 860 kHz as a function of the point where the stub is connected to the skywire. Evidently the stub performs best when connected about 50 m from the tower, and the max-to-min ratio rises sharply as the stub is moved away from this position. The current distribution on the nine tower power line is similar to that on the three tower line of Fig. 2.2, and shows that the best connection point is also the location of the sharp minimum in the current on the skywire. Such a "current zero" is a high impedance point on the transmission line.

Fig. 2.7 examines the effect of stub length when the stub

is placed in the best position from Fig. 2.6. The max-to-min ratio has minimum at an "optimum" length, and the max-to-min ratio rises rapidly as the stub length is changed.

2.3 Conclusion

It has been shown that a power line can be effectively detuned in the MF band by connecting a "detuning stub" to the skywire. The sensitivity of the pattern perturbation expressed as max-to-min ratio has been investigated as a function of the design of the stub. It has been shown that a straight stub and a bent stub are equally good, although the latter is the most promising for implementation on real power lines. The stub is effective because it is a low impedance element connected to a high impedance point on the resonant power line.

3. Frequency Dependence From 200 To 1100 kHz

As proposed by Jones(2), the five tower power line configuration shown in Fig. 3.1 was used to study the resonant behavior over the frequency range of 200 to 1100 kHz. The numerical solution of the Pocklington Integral Equation by the NEC computer code tends to break down in the one wavelength resonance region, and this difficulty is discussed before the frequency dependence of the re-radiation effect on the azimuth pattern is presented. A new parameter called the "integrated current" is defined and used as an alternative to the max-to-min ratio to study the resonances of the power line. Polar plots of the azimuth pattern in both the one and two wavelength resonance regions are presented, and the distribution of RF current corresponding to each resonant mode is discussed.

3.1 Convergence of the Solution

The RF currents flowing over the wires of the power line are determined by an approximate solution of Pocklington's Integral Equation, which expresses the boundary condition that the total axial field along each of the wires must be zero. This integral equation is reduced to a matrix equation by dividing each wire into "segments", and the RF current amplitude and phase on each segment becomes one unknown in the matrix equation that is obtained. The number of segments to be used on a given wire is determined by "rules of thumb" which state that :

- i) segments should be shorter than one tenth of a wavelength, and a length of one-twentieth is usually short

- enough ;
- ii) segments should not be so short that the ratio of the length of the segment to its diameter is less than ten ; and
 - iii) segments on two wires that form a junction should be comparable in length.

A good "confidence check" of the solution can be made by obtaining a solution with a number of segments chosen according to these rules, then doubling the number of segments, and obtaining a second solution. This tests the mathematical property of "convergence", being that as the number of segments is increased the solution should tend to become constant and independent of the number of segments, provided that rule (ii) is not violated. Thus if doubling the number of segments results in little change in the solution, then greater confidence can be placed in the result. However, if a large change results, then the solution must be treated with healthy skepticism, although not rejected entirely.

A simple assessment of the "convergence" of the numerical solution can be made by graphing a convenient parameter of the solution against the number of segments. Thus Fig. 3.2 shows the max-to-min ratio of the azimuth pattern as a function of the number of segments at five frequencies. The ideal result would be a horizontal line at high numbers of segments, and is obtained nearly enough at 350 and 1260 kHz. At 450 and 840 kHz, the solution changes by about five percent for each increase of 100 segments, and these cases are typical of the behavior that must be considered acceptable. However at the one wavelength resonant frequency of 420 kHz the max-to-min ratio changes rapidly with the number of segments. A further increase beyond 300 segments violates rule (ii) given above. The reason for the difficulty with convergence is associated with a mathematical limitation of Pocklington's Equation. For the present purposes, the convergence study in Fig. 3.2 points out that the precise values of RF current, azimuth radiated field and max-to-min ratio must be treated with caution near the one wavelength resonant frequency of 420 kHz, but the solution is satisfactory at 360 and 450 kHz.

Fig. 3.3 shows the changes in the azimuth pattern that are encountered as the number of segments increases at the troublesome frequency of 420 kHz. The change seen with an increase from 50 to 100 total segments is quite substantial, but the changes that come about by increasing the number of segments from 100 to 200 to 300 are not large and mainly consist of the deepening of the minimum at 180 degrees azimuth. The qualitative nature of the patterns remains the same.

Thus the assessment of convergence provides a "confidence check" in the solution. The poor convergence at 420 kHz is indicative of a limitation in the method in the region of 420 kHz, but does not mean that the solution is useless.

Instead, the precise numerical results must be interpreted cautiously but the qualitative effect of the presence of a resonance is indisputable and so a considerably perturbed radiation pattern is expected.

3.2 Verification Against Measured Results

Fig. 3.4 compares the computed azimuth patterns with the measurements of Lavrench and Dunn(5) at 515 and 860 kHz. The power line has thirteen towers for both the measurements and the computations.

At 515 kHz as shown in Fig. 3.4(a), the main difference between the measured and the computed azimuth pattern is the depth of the minima, which are much deeper in the measurement. The frequency of the measurement for Fig. 3.4 was chosen to give the largest max-to-min ratio, and so the measurement model is at resonance. As shown in Fig. 2.4 of Reference (1) the computer model with 9 towers has its "one wavelength transmission line" resonant frequency at about 520 kHz, and is somewhat above resonance at 530 kHz. It would be of interest to compare the frequency dependence of the measured patterns with the computed results in the one wavelength resonance region. Fig. 3.4(b) shows the comparison of the measured and computed patterns at the two wavelength resonant frequency of 860 kHz. The agreement is satisfactory.

3.3 Frequency Dependence

3.3.1 Max-to-Min Ratio

Fig. 3.5 shows the max-to-min ratio of the azimuth pattern from 200 to 1100 kHz. There are two distinct resonance regions, extending from 390 to 510 kHz for "one wavelength resonance" and 790 to 990 kHz for "two wavelength resonance" where these limits have been chosen for a max-to-min ratio of 3 dB. These resonance regions are separated by extensive frequency bands in which the power line is non-resonant and the azimuth pattern is nearly circular.

The one-wavelength resonance band is characterized by two closely spaced peaks at about 420 kHz and an isolated peak at 480 kHz. The resonance mode of the pair of peaks will be termed "one wavelength loop resonance". The RF current distributions are discussed in Sect. 3.4 below. It was indicated above that the numerical solution converges poorly in this frequency range, and so the max-to-min ratio computed with a total of 300 segments is also shown. It is qualitatively the same, and shows sharper peaks at a slightly lower frequency. The isolated peak

at 480 kHz has an RF current distribution which will be termed "two wavelength double-loop" resonance.

The two wavelength resonance region is characterized by a broad peak at 840 kHz for the five tower power line, and a gradual roll off of the max-to-min ratio above this frequency. The RF current mode of the peak at 840 kHz is "two wavelength loop resonance", and a second resonance mode at 940 kHz exists, which has an RF current mode called "four wavelength double-loop resonance" and is discussed further below.

Above 1000 kHz the pattern is nearly circular. At frequencies above 1200 kHz, the monopole antenna illuminating the power line becomes taller than three-quarters of a wavelength and radiates poorly in the azimuth plane, and so the azimuth pattern becomes dominated by the weak re-radiated fields and the max-to-min ratio of this low level pattern is large. It is of little interest to study the azimuth pattern resulting from such a tall broadcast antenna, which would not be used in practice.

The use of a parameter directly related to RF current to reveal the resonances is dealt with next.

3.3.2 The Integrated Current

A parameter directly based on RF current which is suitable for assessing the effect of re-radiation on the azimuth pattern can be defined by noting that the strength of the azimuth field radiated by a vertical wire of length "L" carrying complex current $I(z)$ is proportional to the integral

$$\mathcal{I} = \int I(z) dz$$

which will be termed the "integrated current" for the wire. By comparing the integrated current due to a tower to that due to the broadcast antenna, the possible effect of the tower current on the azimuth pattern can be assessed. Thus if the tower's integrated current is 0.2 of that flowing on the broadcast antenna, then at an azimuth angle where both fields arrive in phase, the net field would be 1.2 times that of the broadcast antenna alone, and if the fields arrive in phase opposition, the net field would be 0.8 of the antenna's. Thus the worst case max-to-min ratio for the pattern of the antenna plus the one tower would be $20 \log(1.2/0.8) = 3.5$ dB. Evidently the ratio of the integrated current on a tower to the integrated current on the antenna, or "integrated current ratio", is a useful parameter for assessing the possible effect of re-radiation.

Fig. 3.6 compares the base current on the broadcast

monopole to the integrated current. With the one volt excitation used, the base current is equal to the admittance of the broadcast antenna in the presence of the five tower power line. As expected the broadcast monopole has a resonance at about 350 kHz where it is about one-quarter wavelength high, and at 1100 kHz where it is about three quarters of a wavelength in height. The integrated current has similar peaks but the maximum at 1100 kHz is much smaller because much of the power is radiated into the elevation plane at this frequency. The integrated current reflects only the fields radiated into the azimuth plane.

Fig. 3.7 uses the integrated current ratio to show the resonances of the five tower power line. The ratio is of the integrated current on the center tower to that on the broadcast antenna. In comparison to the max-to-min ratio graph of Fig. 3.5, the two resonance regions are present, although their structure is somewhat different. In the one-wavelength region the convergence of the numerical solution is worrisome for the integrated currents as it was for the max-to-min ratio, which is, of course, derived from the same currents. Thus the figure compares the solutions with 100 and 300 segments on the power line. Only one peak is seen in Fig. 3.7 at 420 kHz for "one wavelength loop resonance". The peak at 480 kHz corresponding to "two wavelength double-loop resonance" is present. The two wavelength resonance region is characterized by two equal peaks corresponding to "two wavelength loop resonance" at 850 kHz, and "four wavelength double-loop resonance" at 950 kHz.

The next two sections report on the azimuth pattern and the RF current distribution throughout this frequency range.

3.4 Azimuth Pattern as a Function of Frequency

Below the start of the one wavelength resonance region at 380 kHz, the azimuth pattern is almost circular. Fig. 3.8 shows the changes in the azimuth pattern throughout the one wavelength resonance region. At 400 kHz, there is a minimum at zero degrees azimuth, and a maximum at 180 degrees. These quickly change to a peak at zero degrees and a minimum at 180 degrees, at 420 kHz. Above 420 kHz, the lobe at zero degrees azimuth grows relative to the remainder of the pattern, becoming quite pronounced at 480 kHz. At 500 kHz the pattern is returning to circular, and becomes highly so at higher frequencies until the two-wavelength resonance region is encountered.

Fig. 3.9 shows the pattern throughout the two wavelength resonance region. The pattern is characterized by maxima at about 50 and 150 degrees and minima at about 30 and 130 degrees. These features increase in intensity up to 840 kHz then gradually smooth out with increasing frequency. At 1000 kHz the

pattern is a circle with ripples of small amplitude due to re-radiation. The patterns become increasingly circular up to 1100 kHz.

3.5 RF Current Distribution and Resonance Modes

This section displays the RF current distribution on the towers and skywires in the format of Fig. 3.10 at 200 kHz. At the left the magnitude and phase of the current at two points on each of the five towers is given. Thus for each tower the left point is located at a distance of one-quarter the tower height or 12.6 m above the tower base, and the right hand point at 37.9 m above the base. In Fig. 3.10, the center tower carries the strongest current, which is about twice as strong as the current on the end towers. Note the current scale of 40 microamps. The three center tower currents are at a phase of minus ninety degrees relative to the one volt, zero phase excitation of the broadcast antenna. The end towers are at a phase of about minus forty-five degrees. The right hand portion of the figure shows the current on the four skywires interconnecting the towers. The current has a strong travelling wave component, exhibited by the phase behavior, which varies roughly linearly with distance along the skywires. This "travelling wave" behavior is characteristic of non-resonant skywire currents.

Fig. 3.11 shows the RF current distribution that exists on the towers and skywires at "one wavelength loop resonance" at 420 kHz. The tower currents are all in phase, and the three center towers carry currents twice as strong as the end towers. The skywire currents are pure standing waves, have constant-phase-with-distance, and exhibit zero current at the skywire centers with corresponding sharp 180 degree phase reversals.

Fig. 3.12 shows the RF current distribution at 460 kHz, in the trough between one wavelength loop resonance and the two wavelength double-loop resonance mode discussed below. The center loops are not resonant but the two end loops carry typically resonant current distributions.

Fig. 3.13 shows the current distribution at 480 kHz and illustrates "two wavelength double-loop resonance". Here the resonant path consists of a tower, the skywire to the second tower, that tower and a return path in ground. This path spans two loops and is of length $(2 \times 50.9 + 2 \times 274) \times 2 = 1300$ m and is two wavelengths long at 462 kHz, which is reasonably near the 480 kHz value evident in the computed results. The current distribution is similar to the familiar RF current for two wavelength loop resonance, except spread across two skywires of the power line, and is sketched in Fig. 3.14. In this

double-loop mode a minimum in the current is expected at about 40 percent of the tower spacing from one tower, then again at about 60 percent of the spacing on the next skywire, and is clearly seen in Fig. 3.13. The important difference between the modes of Fig. 3.11 and 3.13 is that in the former the current has a minimum at the skywire center, while in the latter the minima are shifted from the center.

Fig. 3.15 shows the RF current distribution at the non-resonance frequency of 700 kHz. The magnitude of the current is much smaller than in Fig. 3.13, because the scale is changed from 6000 microamps to 350 microamps. Note the linear-phase-with-distance behavior.

Fig. 3.16 shows the RF current distribution of "two-wavelength loop resonance" at 840 kHz. Here the path of a tower, the skywire to the next tower, that tower, and the return path in ground is two wavelengths long. Adjacent tower currents differ in phase by 180 degrees, and the skywire current exhibits constant phase with distance behavior, and abrupt phase reversals at minima in the current. The skywire current has a maximum at the skywire center, and sharp minima near each tower.

Fig. 3.17 illustrates the mode of "four wavelength double-loop resonance". Here a two-loop path is about four wavelengths long and the current distribution can be idealized as in Fig. 3.18. Thus three peaks and four minima are expected across two skywires. Also, the minima are unsymmetric with respect to the center of a skywire, but are symmetric about the center tower of the double loop. This behavior is evident in Fig. 3.17.

Fig. 3.19 shows the RF current at the top end of the frequency band under study, at 1100 kHz. The current is typically non-resonant.

3.6 Resonance Chart

Fig. 3.20 is a resonance chart which gives the frequencies of loop resonance and of double loop resonance for 50.6 m tall towers, as a function of the spacing of the towers. The mode described here as "double-loop" resonance was termed "hybrid" resonance in Reference (1). The frequency sweep for nine towers of Fig. 2.4 of Reference (1) shows that with nine towers the one wavelength loop resonance is present at 420 kHz, the two wavelength double loop resonance at 480 kHz, and in addition a weaker third peak is present at 520 kHz which appears to correspond to the "transmission line" resonance mode. This latter is not evident with a five tower power line.

3.7 Summary

This chapter has investigated the resonant modes of a five tower power line and identified a one-wavelength and a two-wavelength resonance region. Each region exhibits two important resonant modes, one of which is a simple loop resonance and the other a resonance mode across two loops. The azimuth patterns in each resonance region have been presented and the RF current distribution has been exhibited for each mode.

It should be emphasized that this study has involved one very specific excitation, and that the results would differ if another excitation were used. In particular, it is expected that the frequencies of resonance of the power line are independent of the excitation, and that the resonant modes described could be excited with other broadcast antenna configurations. However, there may be other resonance modes at other frequencies which are excited strongly by other types of broadcast antenna, and which are only weakly exhibited in the present study.

4. Preliminary Study with Finite Ground Conductivity

In this initial study a 640 foot monopole antenna over an eight radial ground screen was used to illuminate a three tower power line, using the 166 foot tower height and 900 foot tower spacing derived from the Hornby site. In the following, the RF currents on this structure and the azimuth and elevation patterns are compared for four cases, namely : (i) no ground at all (zero conductivity) ; (ii) perfect ground using the method of images ; (iii) finite conductivity ground using the Sommerfeld-Norton model with "typical" permittivity and conductivity values provided by the CBC ; and (iv) the Fresnel reflection coefficient model for lossy ground. The Sommerfeld-Norton ground ("SN ground") uses the Sommerfeld integrals for ground fields when the interaction distance is small and Norton's asymptotic approximations for larger distances(6,7). It is a rigorously correct mathematical model for structures entirely above the ground. For wires that connect to the ground, the NEC computer code assumes that the derivative of the current with respect to distance along the wire is zero at the connection point to ground, in order to obtain a boundary condition necessary for the solution to proceed. This assumption is rigorously correct only for a perfect ground, but is considered quite reasonable for modelling the bases of those hydro towers which are well grounded.

The Fresnel ground uses plane wave reflection coefficients

to compute the interaction of segments above a lossy ground, and is not rigorously valid for segments close to or connected to ground.

4.1 The Monopole and Ground Screen

A 640 foot monopole over a ground screen of eight radial wires was used as a source antenna, as shown in Fig. 4.1. The radials were uniformly spaced and chosen to be 0.4 wavelengths long at the operating frequency of 860 kHz. The antenna was modelled with eight segments and each radial wire with four segments. The computer code does not allow wires to lie below the ground surface at $z=0$, nor in the $z=0$ plane. For this reason the radials of the ground screen were arbitrarily raised to five meters or $5/348$ of the wavelength above the ground(7), although a somewhat closer value is permissible in the program.

Fig. 4.2 shows the elevation pattern of the monopole and eight radials, computed at a distance of 10,000 meters which is 28 wavelengths at 860 kHz. The figure shows that with a ground of zero conductivity and a permittivity and permeability equal to that of free space (ie: no ground) the eight radials are an adequate "ground screen" for the present study, because the pattern is close to that with a perfect ground. However, with the Sommerfeld-Norton ground model with a relative permittivity of 15 and a conductivity of 0.02 mhos/meter, the elevation pattern is quite different. There is a minimum at 45 degrees elevation. Because only the "space wave" and not the "ground wave" is included in the pattern, the field becomes zero as the elevation angle approaches zero (theta approaches ninety degrees)(6,7).

As mentioned above the ground can be modelled using Fresnel reflection coefficients, and Fig. 4.2 shows that the resulting elevation pattern is quite similar to that obtained using the Sommerfeld-Norton model. This was found to be the case throughout this study.

When the ground wave is included in the calculation of the far field, then the field becomes constant as theta approaches ninety degrees, as shown in Fig. 4.3. The ground wave is not readily included in the computation of elevation patterns, due to a limitation of the NEC computer code(6,7).

4.2 Antenna Plus Power Line

A three tower, two loop "power line" was introduced near the antenna as shown in Fig. 4.4, using radii of 3.51 m for the towers and 0.71 m for the skywires, respectively. The elevation

pattern is very similar to that with no power line, and will not be shown. Fig. 4.5 compares the azimuth patterns for the perfect ground, Sommerfeld-Norton ground model, and the Fresnel ground. The field at 10,000 m is stronger when the finite conductivity of ground is modelled than when the perfect ground is used. The patterns with the Sommerfeld-Norton ground and the Fresnel ground are quite similar. Fig. 4.6 compares these patterns with one another by shifting them so that they are at the same level. The pattern with the perfect ground is very close to that with the Fresnel ground, and these are not very different from that with the Sommerfeld-Norton ground model. The max-to-min ratio of the pattern with the SN ground is 1.49 dB, compared to 1.30 dB for the perfect ground or the Fresnel ground.

To compare the methods in terms of running time, note that the SN ground model requires an investment of 220 CPU seconds to generate a table of values from which the Sommerfeld integrals are evaluated, and then a further 308 seconds to compute the RF currents and radiation patterns in the presence of the ground. The table of values can be reused for other configurations at the same frequency with the same ground. The Fresnel ground requires 255 CPU seconds but the perfect ground only 66 seconds. Clearly the perfect ground approximation is quite economical compared to the other models. Also, the rigorous SN ground model requires only 25 percent more running time than the Fresnel model, given the table of values for the evaluation of the Sommerfeld integrals.

4.3 Comparison of the RF Current Distributions

Figs. 4.7 and 4.8 show the RF current distributions with a perfect ground and with the Sommerfeld-Norton ground respectively. Thus Fig. 4.7(a) and 4.8(a) show the current on one radial of the eight wire ground screen and on the monopole, and demonstrate that the ground has little effect on these currents. However, a comparison of Figs 4.7(b) and 4.8(b) show that although the nature of the RF current distribution is similar in both cases, the current is stronger in the presence of the Sommerfeld-Norton ground. This cannot be taken as a general result at present and must be interpreted with caution.

4.4 Summary

This initial investigation of the effect of the finite conductivity of the ground on the re-radiated fields indicates that the radiation patterns in the presence of the imperfect ground will not be greatly different from those computed over a perfectly conducting ground. The investigation must now be

extended to include an assessment of the changes that take place in the resonant frequencies of the power line when the finite conductivity of the ground is included in the computations.

5. Further Work

The following projects are being undertaken at present.

5.1 Detuning

A stub is being designed for the one wavelength resonance band. The response of the power line with stubs in place over the whole frequency band is being determined. The use of shorter, capacitively terminated stubs on the towers is being studied.

5.2 Finite Conductivity Ground

The effect of the finite conductivity of the ground upon the resonant frequencies of the model is being studied. These computations are tedious because the NEC code cannot sweep the frequency for this problem, but must be run at each frequency individually. It would be of interest to investigate the azimuth patterns for a variety of ground parameter values.

REFERENCES

1. C.W. Trueman and S.J. Kubina, "Prediction by Numerical Computation of the Re-Radiation from and the Detuning of Power Transmission Lines," AM Re-Radiation Project Interim Report No. 1, Technical Note No. EMC-80-05, Concordia University, September, 1980.
2. D.E. Jones, Ontario Hydro, private communication.
3. J.S. Belrose, C.W. Trueman, S.J. Kubina, W. Lavrench, and J.G. Dunn, "On Minimizing the Effects of Re-Radiation from Power Transmission Lines on the Radiation Patterns of MF-AM Broadcasting Antenna Arrays," accepted for presentation at the IEE Second International Conference on Antennas and Propagation, University of York, United Kingdom, April 13-16, 1981.
4. W. Lavrench, private communication, Sept. 28, 1980.
5. W. Lavrench and J.G. Dunn, reported in J.S. Belrose, "The Effects of Re-Radiation from Highrise Buildings, Transmission Lines, Towers and Other Structures Upon AM Broadcasting Directional Arrays", Interim Report No. 10, DOC Project No. 4-284-15010, October 9, 1980.
6. G.J. Burke and A.J. Poggio, "Numerical Electromagnetic Code(NEC) - Method of Moments", Technical Document No. 116, prepared for the Naval Electronic Systems Command (ELEX 3041), January 2, 1980.
7. G.J. Burke, E.K. Miller, J.N. Brittingham, D.L. Lager, R.J. Lytle, and J.T. Okada, "Computer Modelling of Antennas Near Ground", Lawrence Livermore Laboratory Technical Report No. UCID-18626, May 13, 1980.

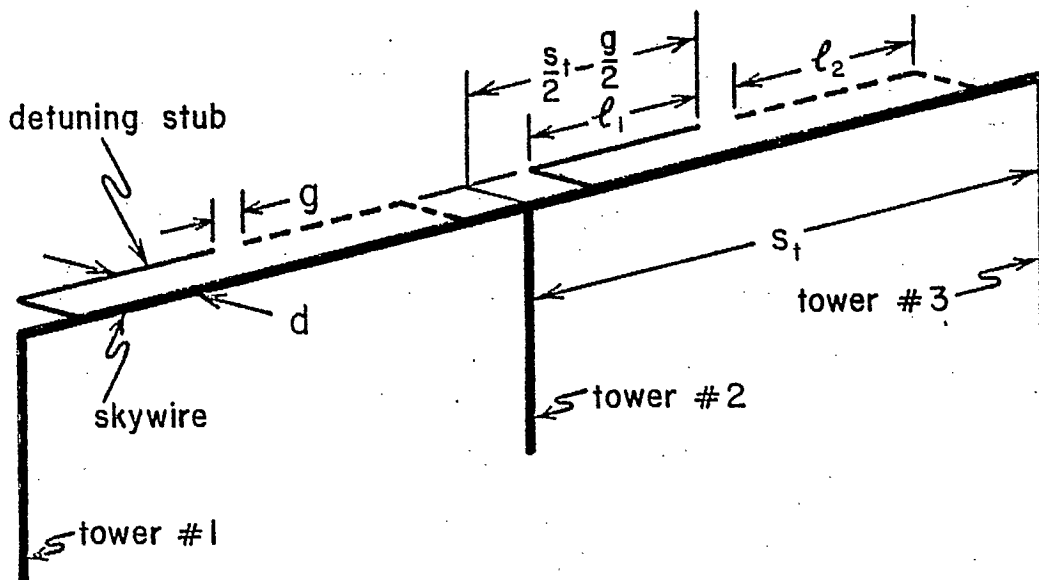


FIGURE 2.1

A "power line" consisting of three towers joined by skywires.

WIRE RADIATOR CURRENT DISTRIBUTION STRAIGHT, EVENLY-SPACED POWER LINE THREE TOWERS, NO STUBS

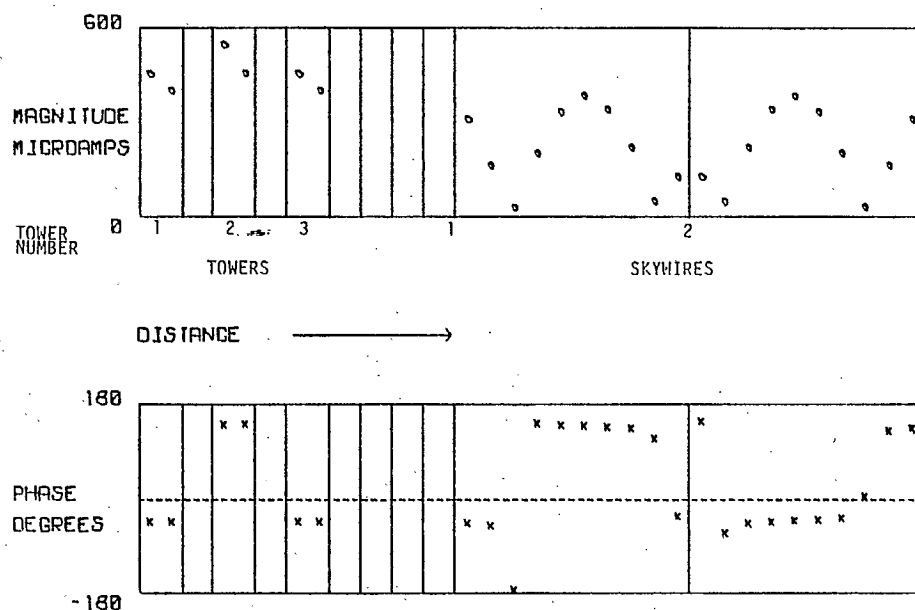


FIGURE 2.2

RF currents on the tower and skywires of the three tower power line with no detuning stubs, at 860 kHz.

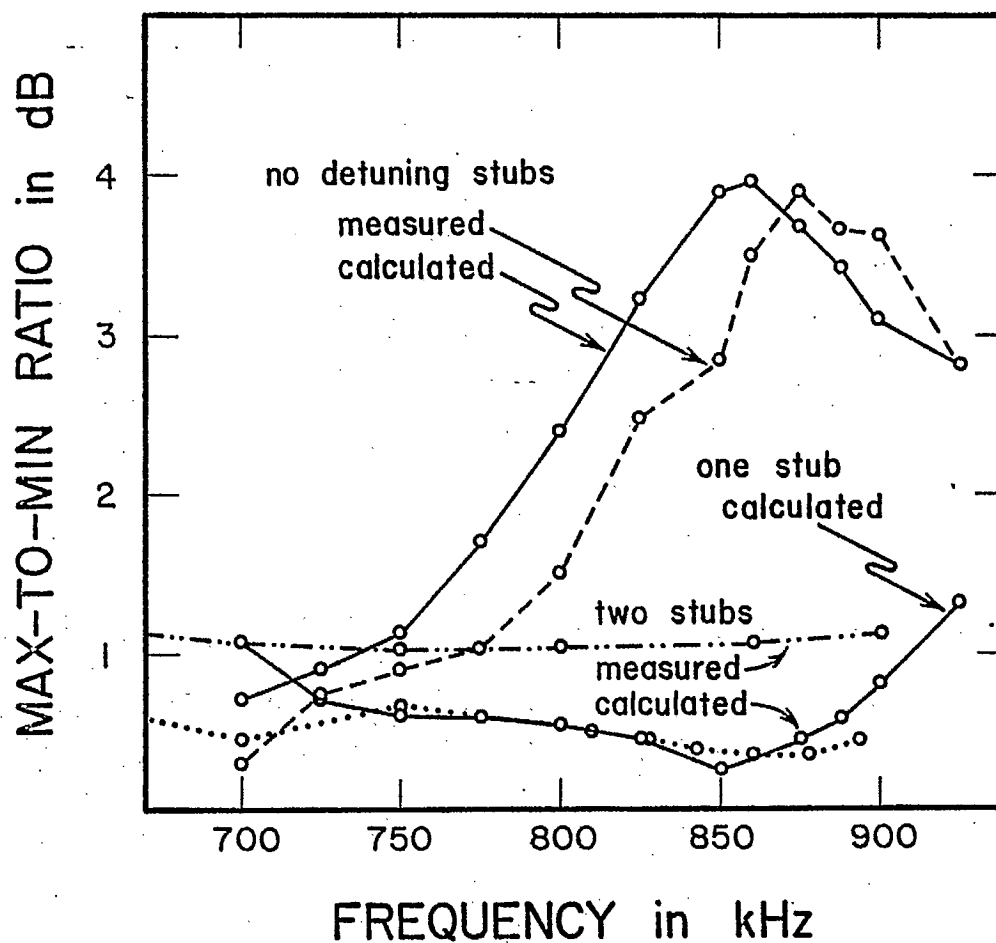


FIGURE 2.3

The max-to-min ratio of the azimuth pattern as a function of frequency for a "power line" of three towers, with no detuning stubs; with one stub on each skywire tuned to 860 kHz; and two stubs on each skywire tuned to 740 kHz and 860 kHz.

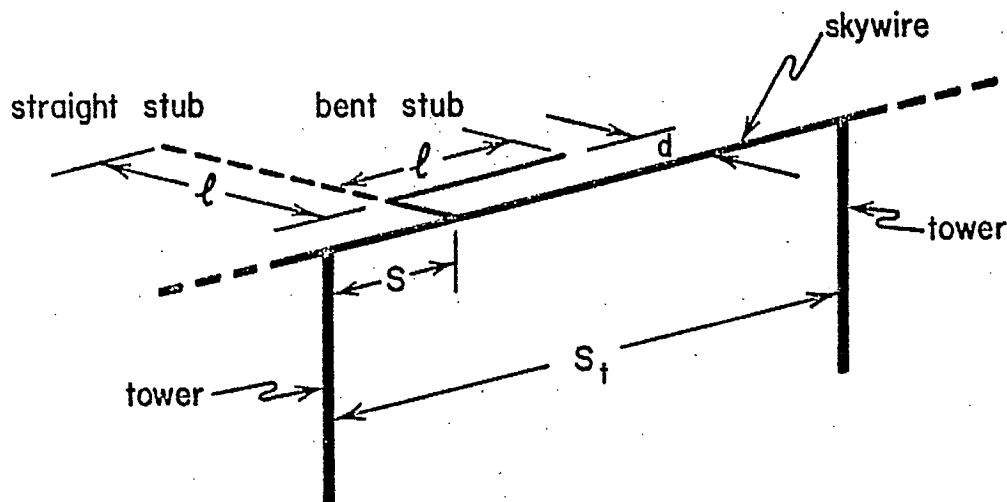


FIGURE 2.4

One pair of towers with skywire, showing the "straight" stub and the "bent" stub configurations. The length of each type of stub is $(l+d)$.

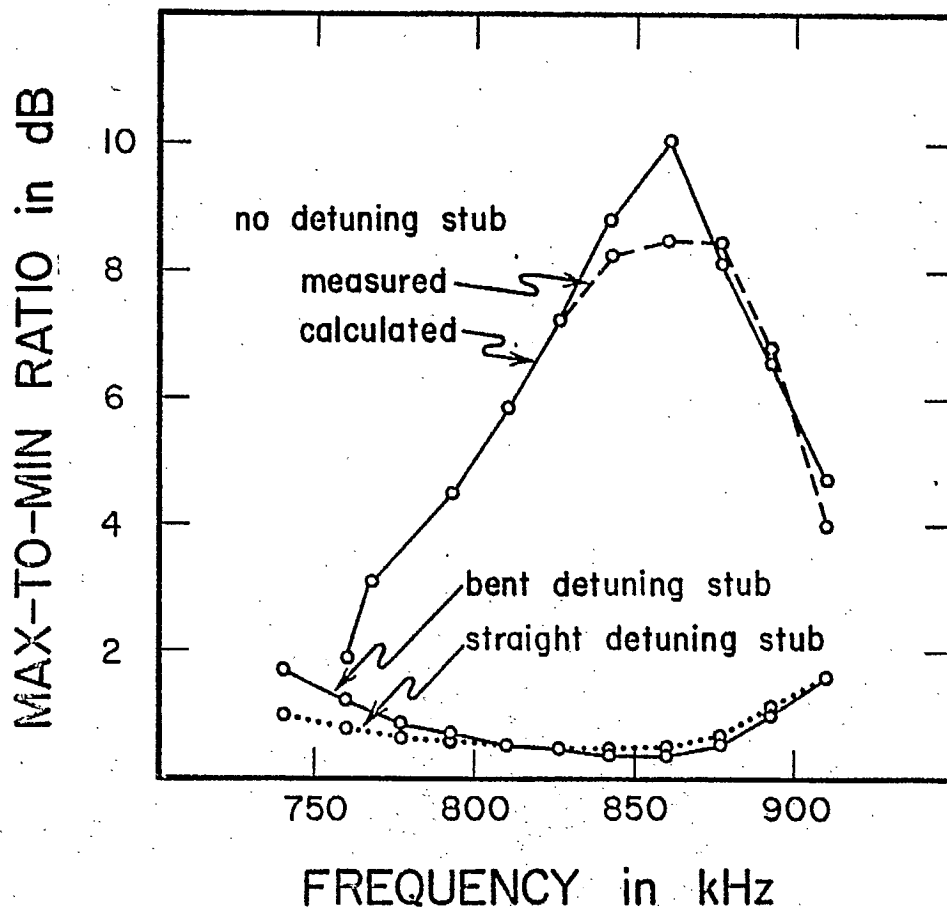


FIGURE 2.5

The max-to-min ratio as a function of frequency for a 9-tower "power line" with no detuning stubs; and with a "straight" and a "bent" stub on each skywire. The length of the "straight" stub is $(l+d) = 115$ m, and its position is $0 = 50$ m. The length of the "bent" stub is $(l+d) = 105$ m and its position is 50 m.

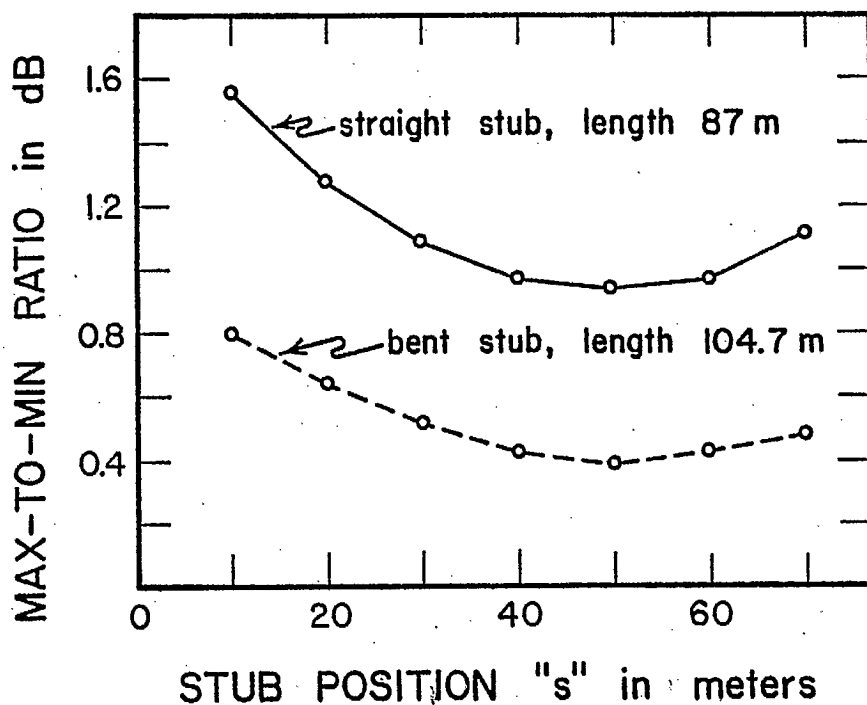


FIGURE 2.6

Max-to-min ratio as a function of stub position for the "straight" and "bent" stub. Note: straight stub was not optimized, see Fig. 2.7.

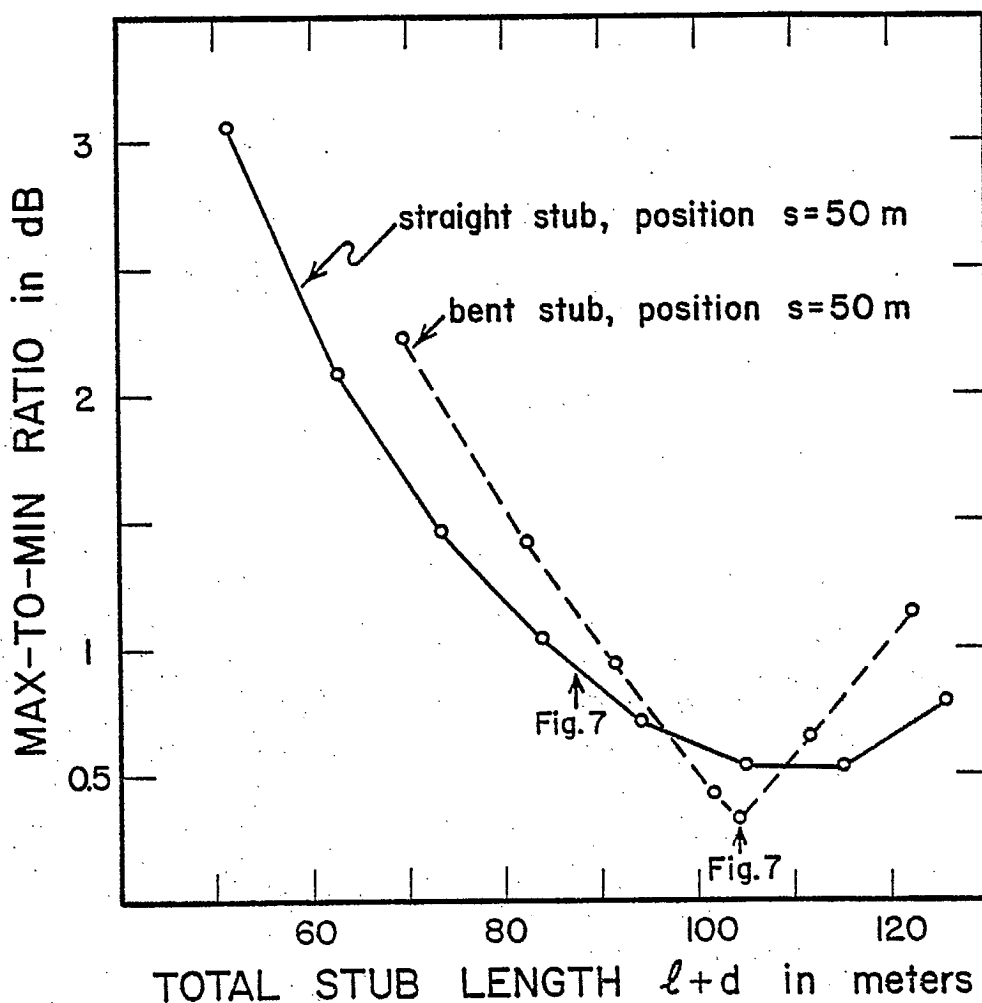


FIGURE 2.7

Max-to-min ratio as a function of the stub length for a fixed s of 50 metres. For "bent" stub, the total length is d plus ℓ .

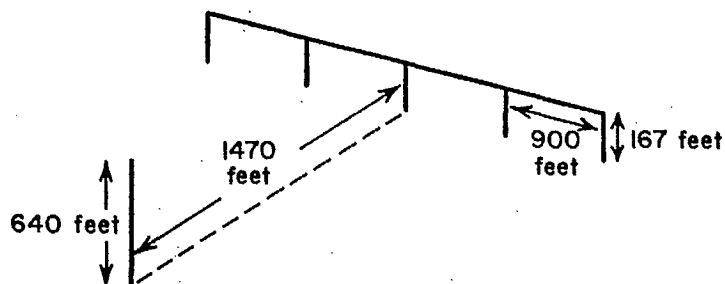


FIGURE 3.1
Dimensions of the problem.

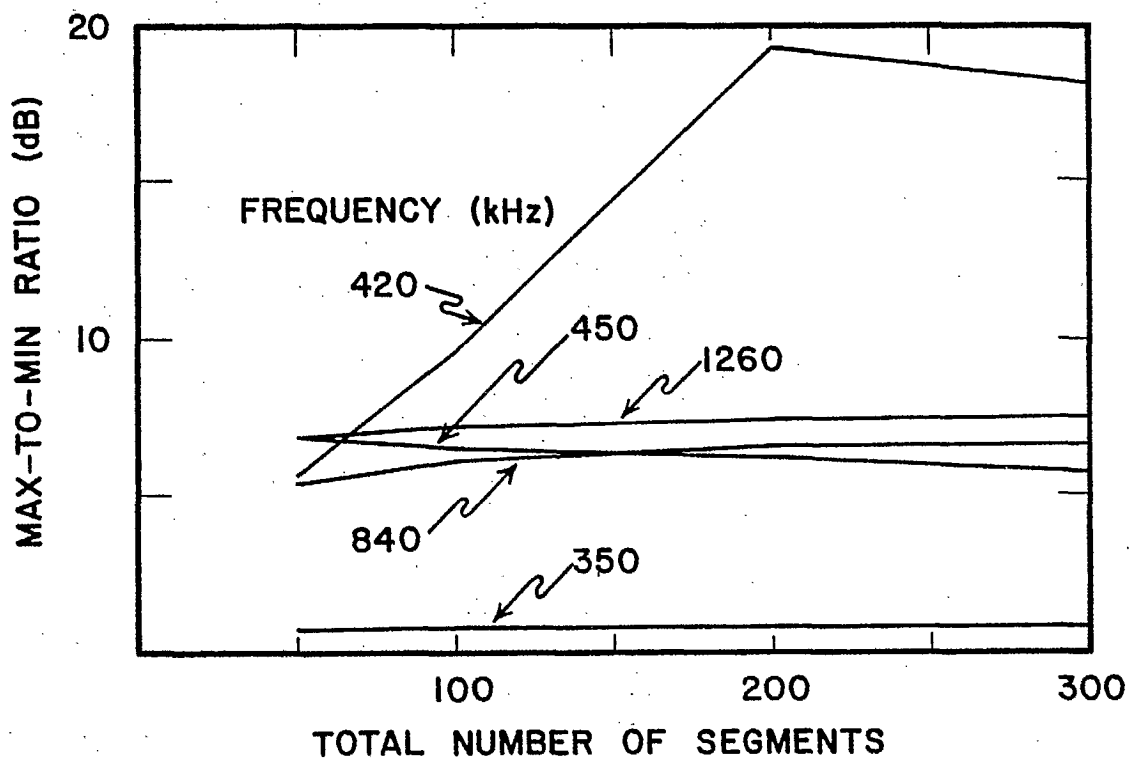
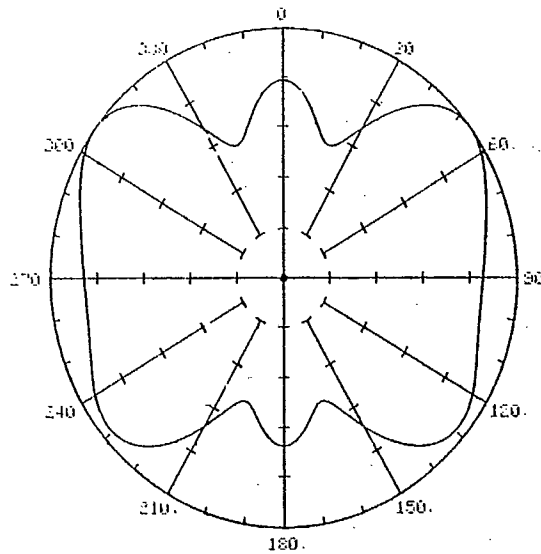


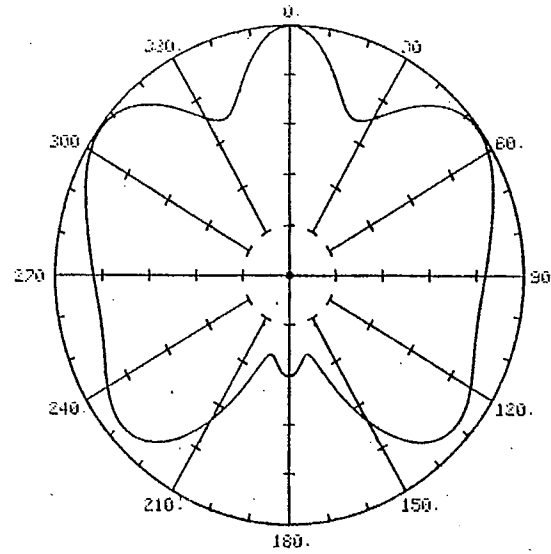
FIGURE 3.2

The "convergence" of the solution expressed by plotting max-to-min ratio as a function of the total number of segments on the model.

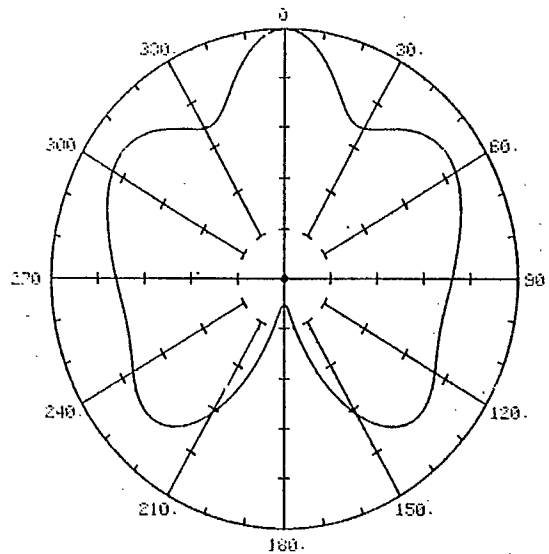
LINEAR SCALE



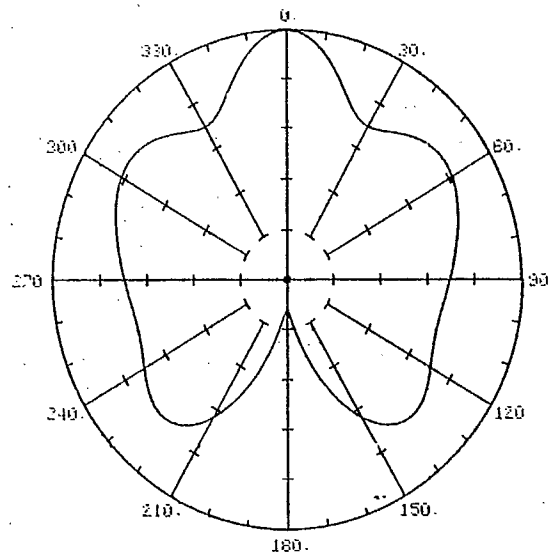
(a) 50 segments



(b) 100 segs



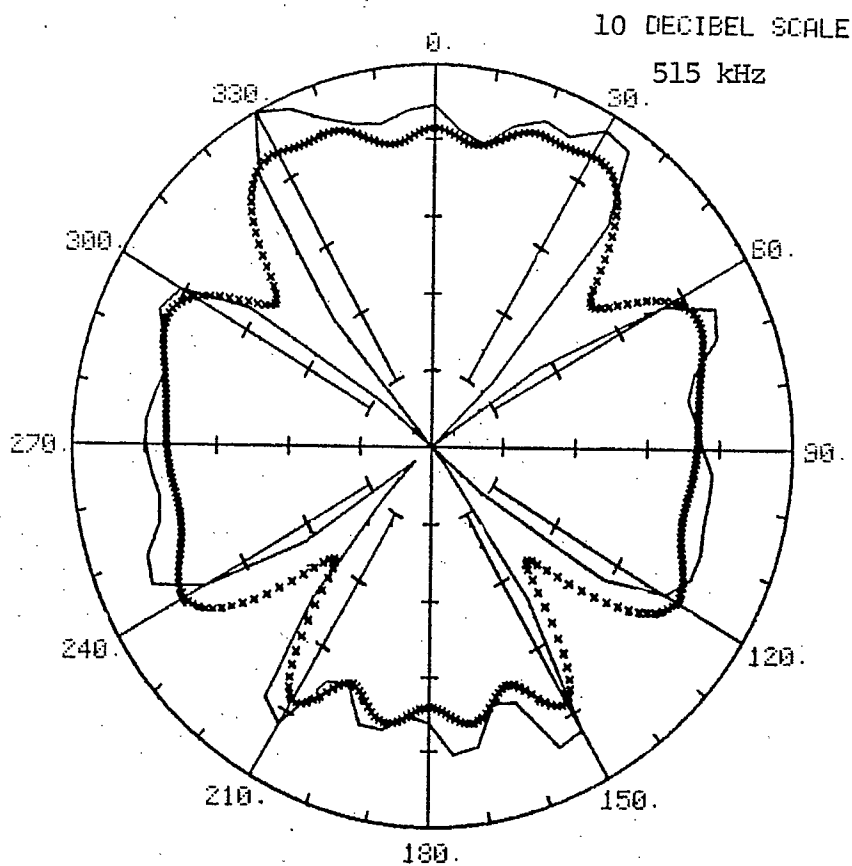
(c) 200 segs



(d) 300 segs

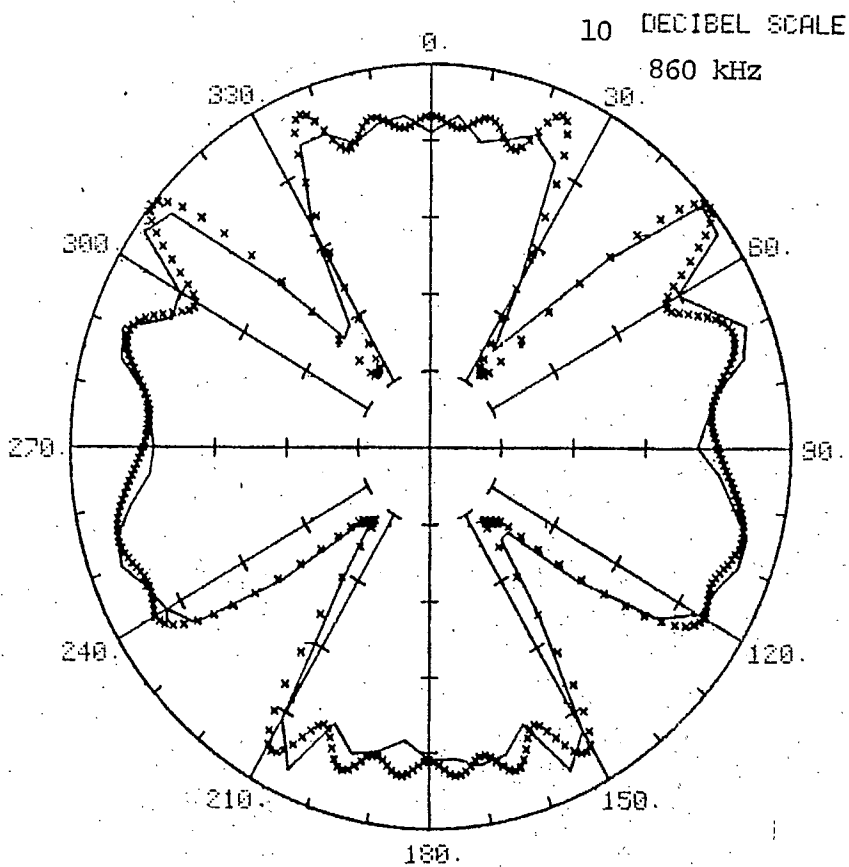
FIGURE 3.3

This figure illustrates the changes that come about in the azimuth pattern at 420 kHz as the number of segments increases.



(a)

FIGURE 3.4
Comparison of
computations and
measurements.



(b)

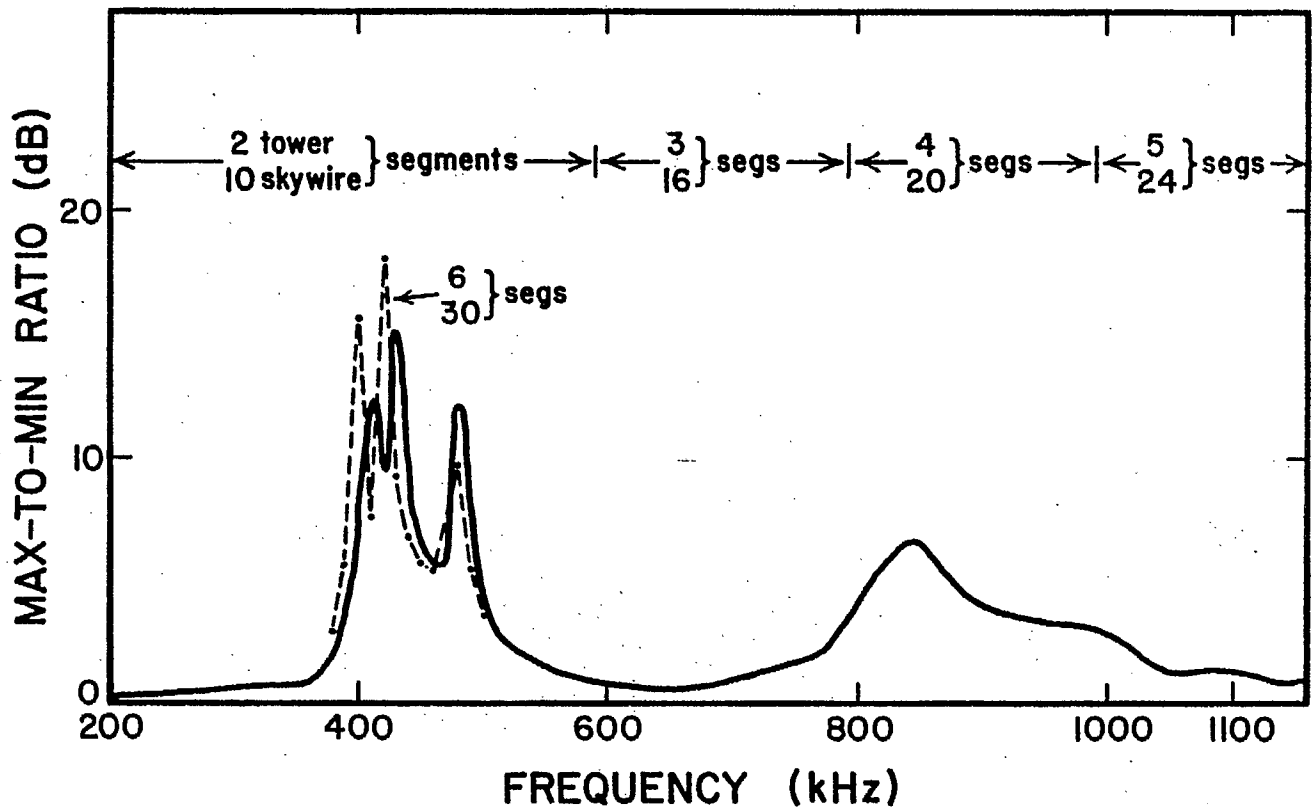
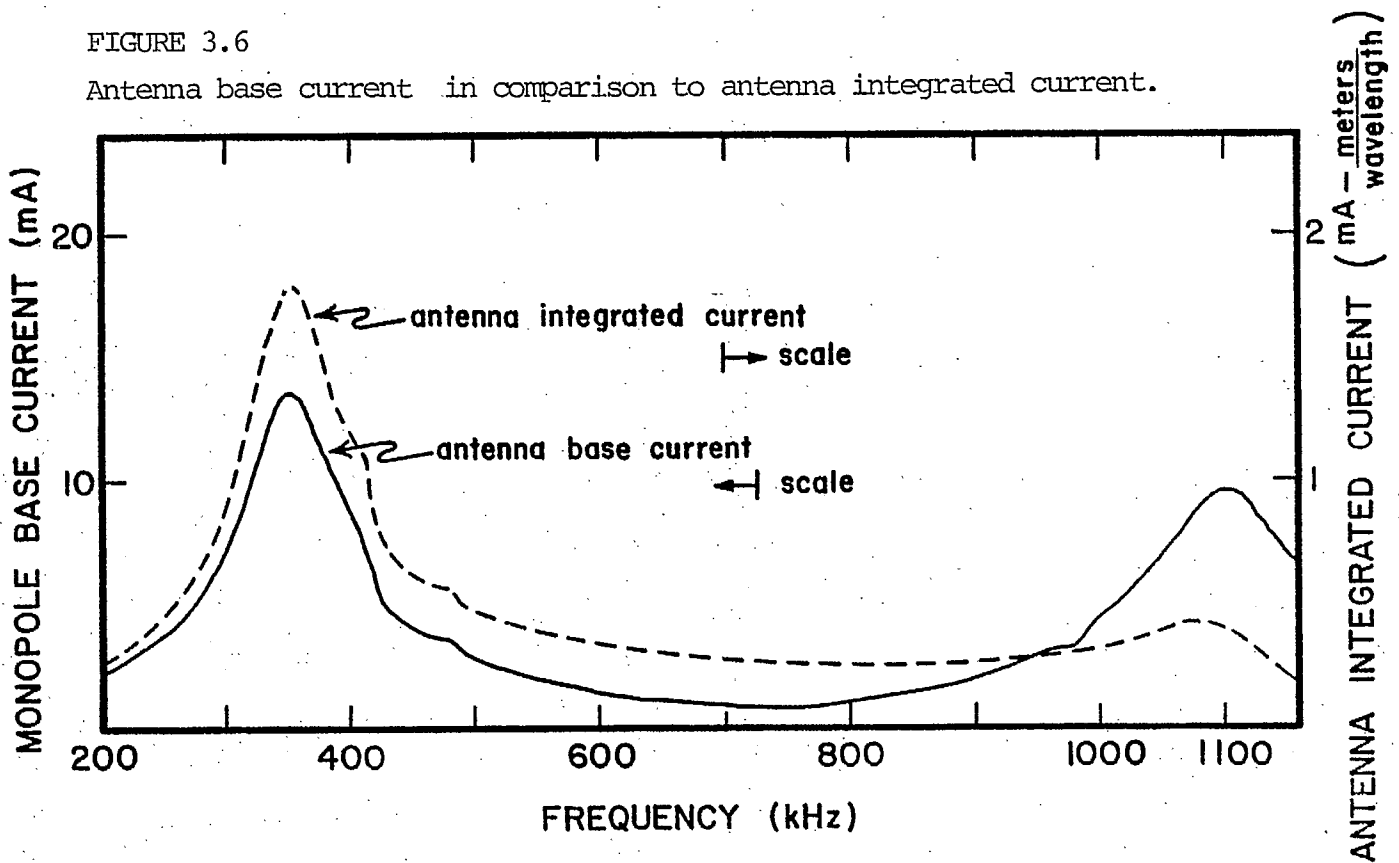


FIGURE 3.5

The power line's resonances revealed by plotting the max-to-min ratio of the azimuth pattern as a function of frequency.

FIGURE 3.6

Antenna base current in comparison to antenna integrated current.



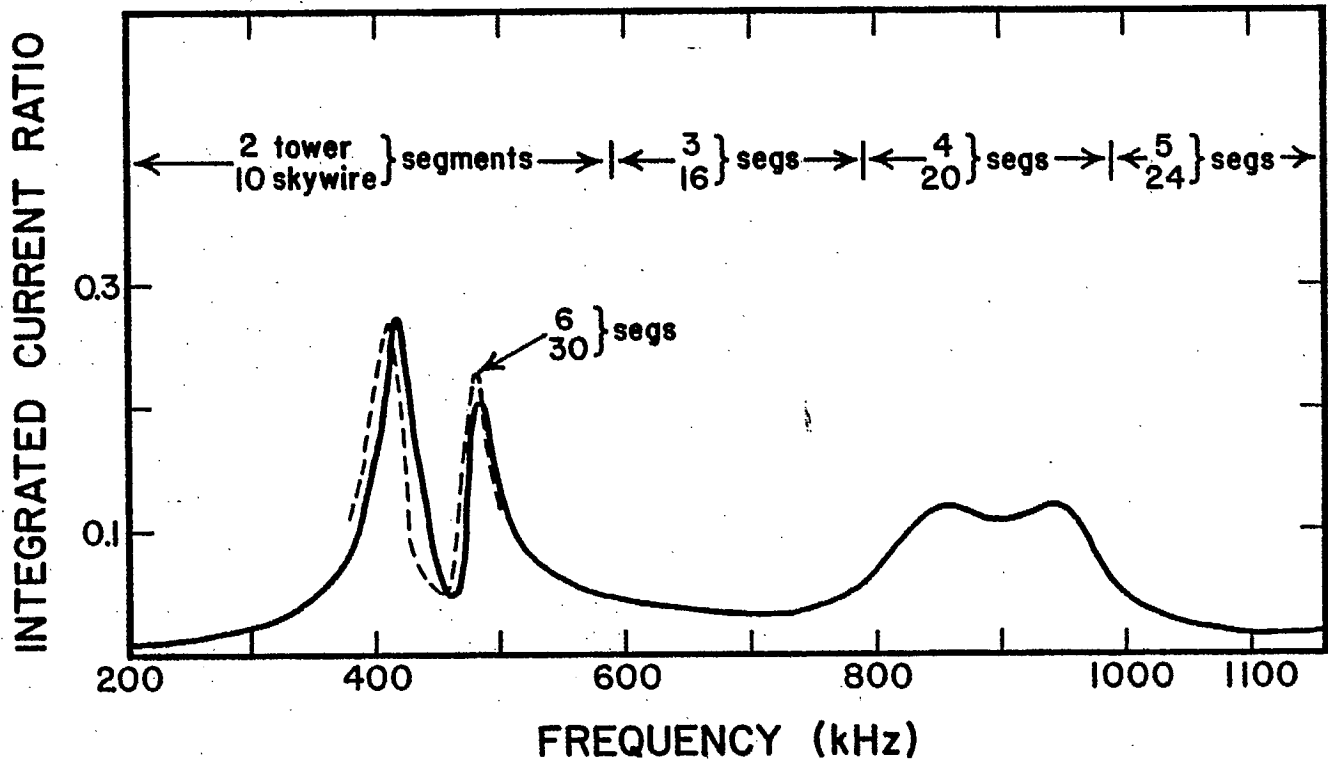
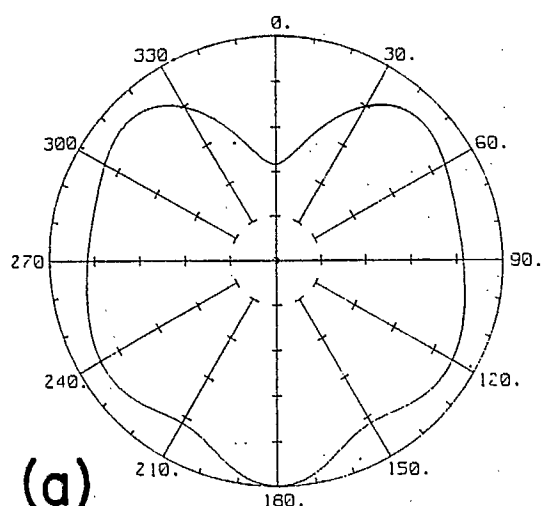


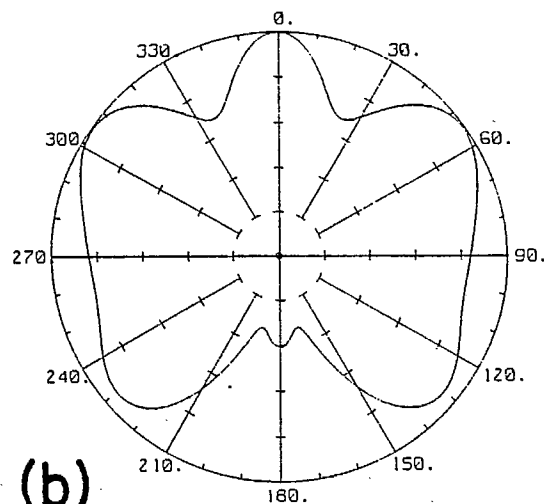
FIGURE 3.7

The power line's resonances revealed by plotting the ratio of the integrated current on the center tower to the integrated current on the broadcast antenna as a function of frequency.



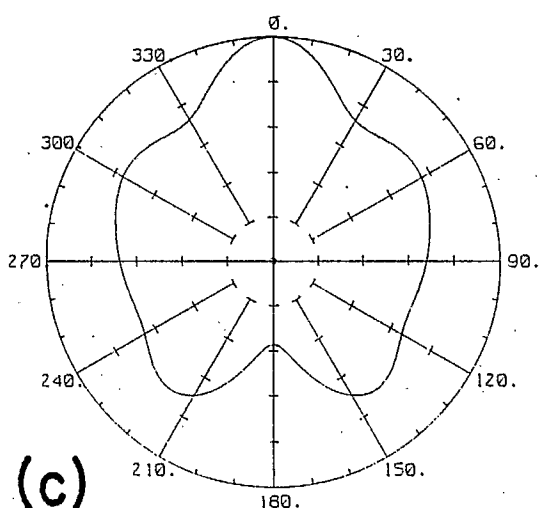
(a)

400 kHz



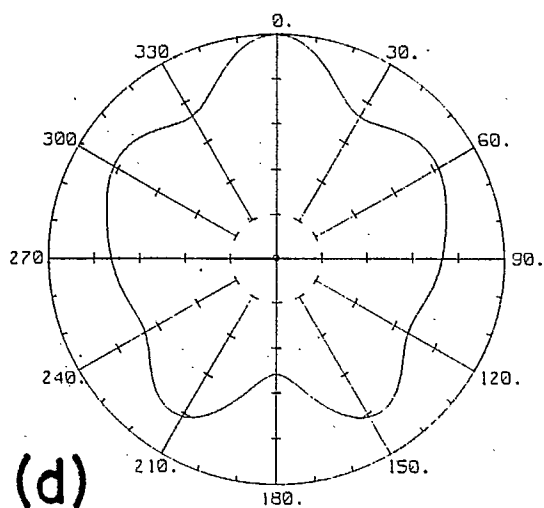
(b)

420 kHz



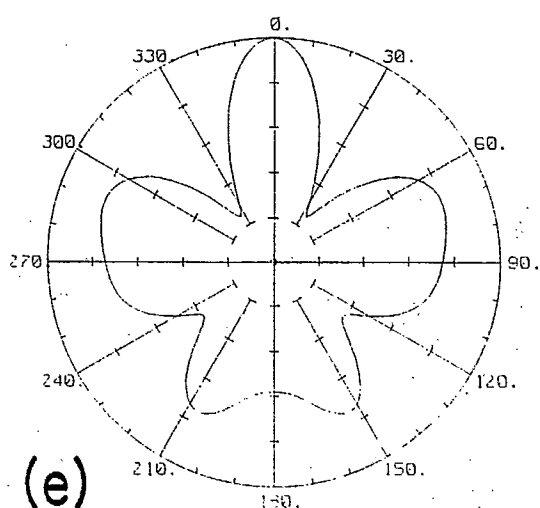
(c)

440 kHz



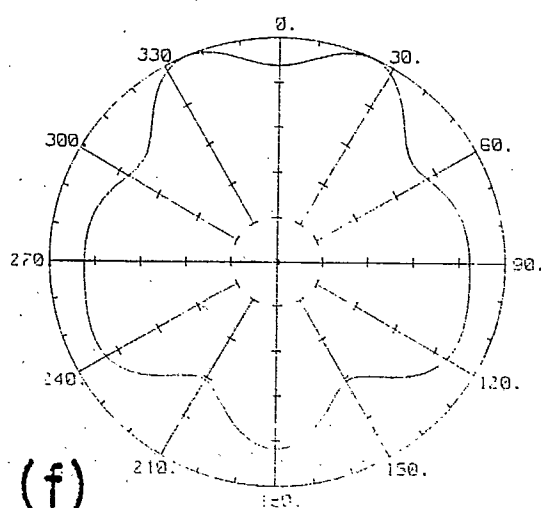
(d)

460 kHz



(e)

480 kHz



(f)

500 kHz

FIGURE 3.8

Azimuth patterns in the one wavelength resonance region.

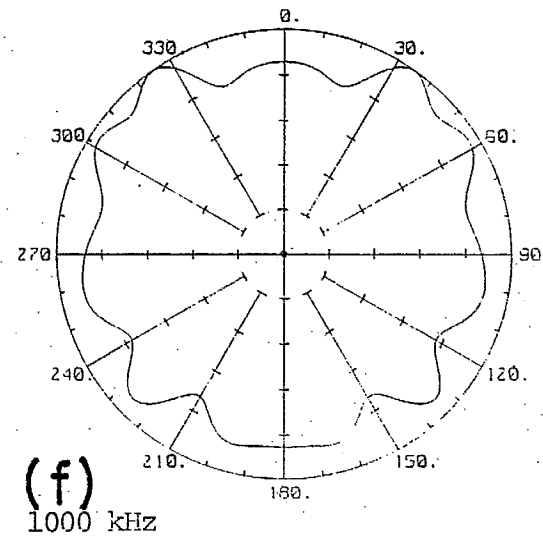
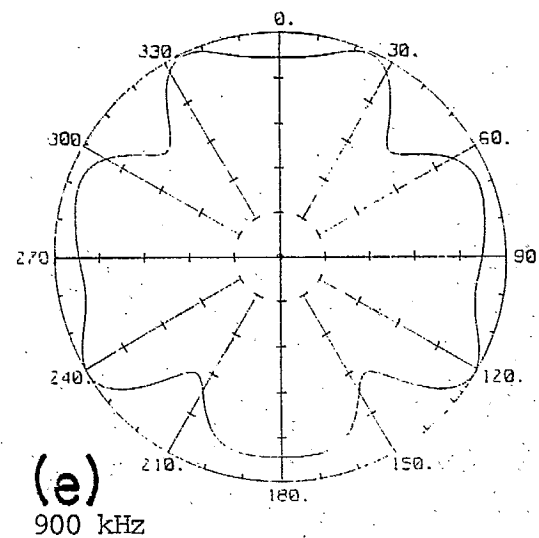
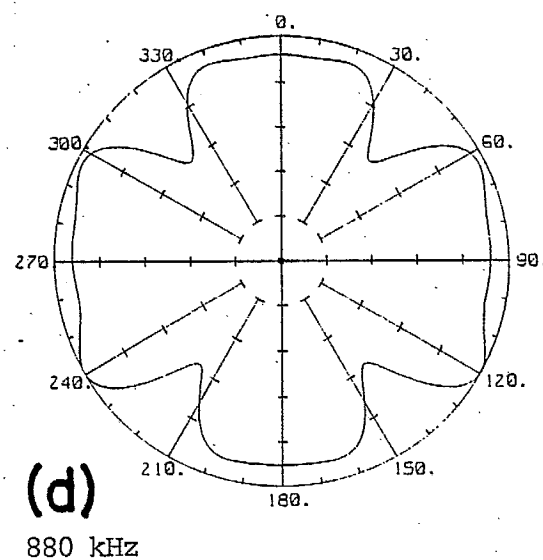
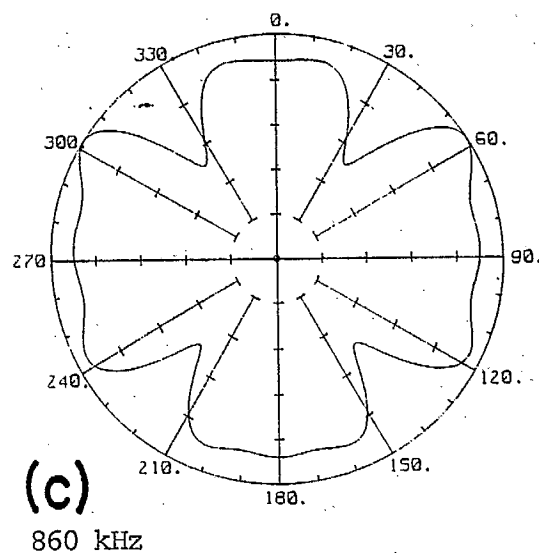
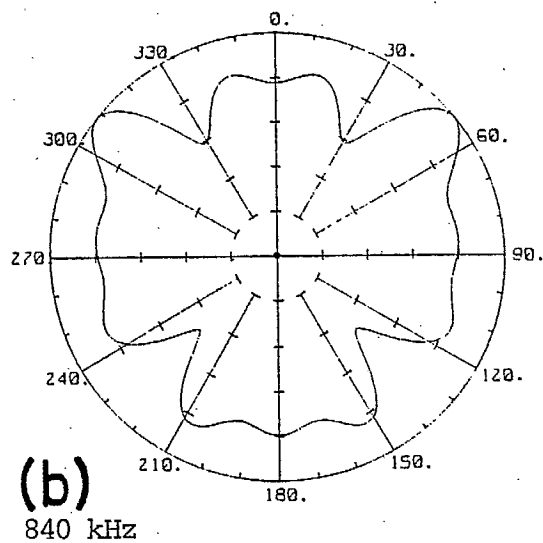
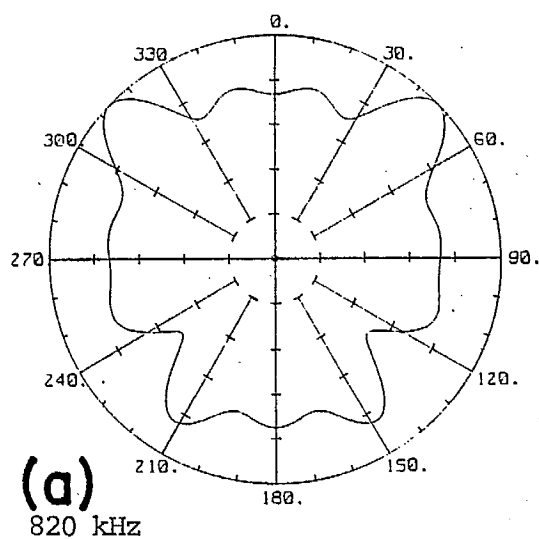


FIGURE 3.9

Azimuth patterns in the two wavelength resonance region.

WIRE RADIATOR CURRENT DISTRIBUTION

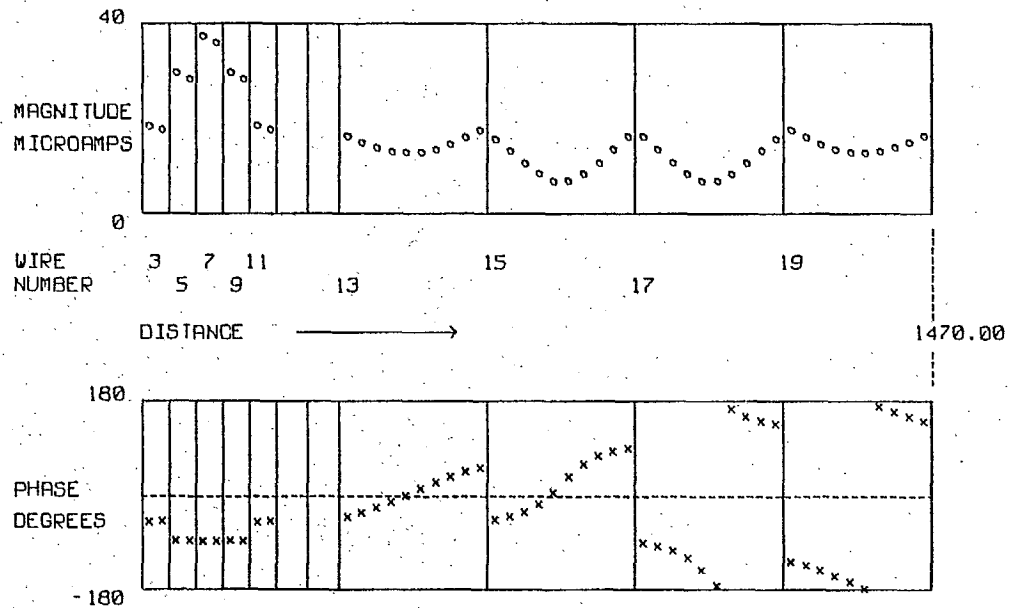


FIGURE 3.10
RF current distribution at 200 kHz.

WIRE RADIATOR CURRENT DISTRIBUTION

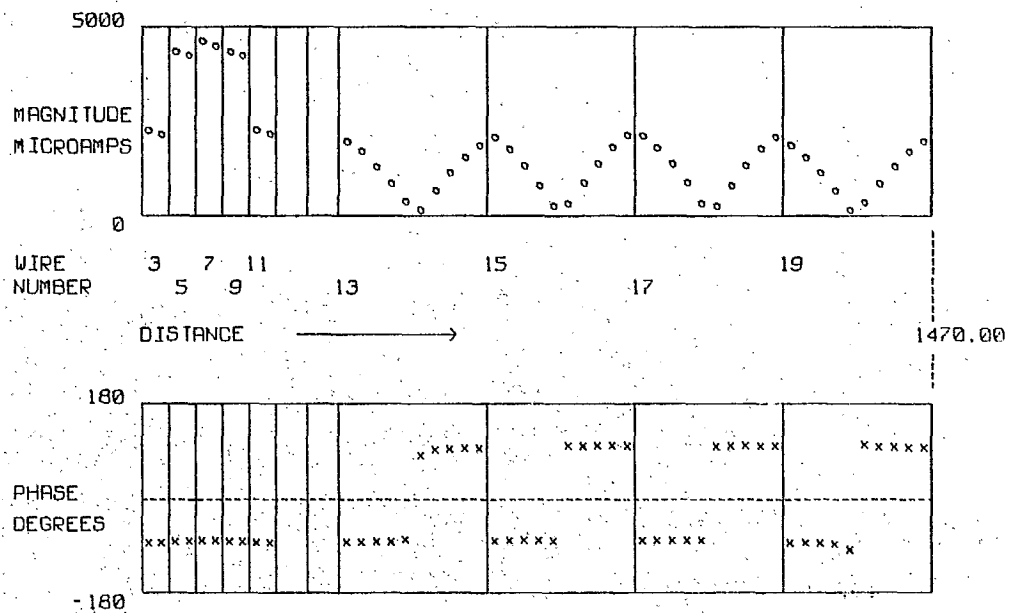


FIGURE 3.11
RF current distribution for "one wavelength loop" resonance at 420 kHz.

WIRE RADIATOR CURRENT DISTRIBUTION

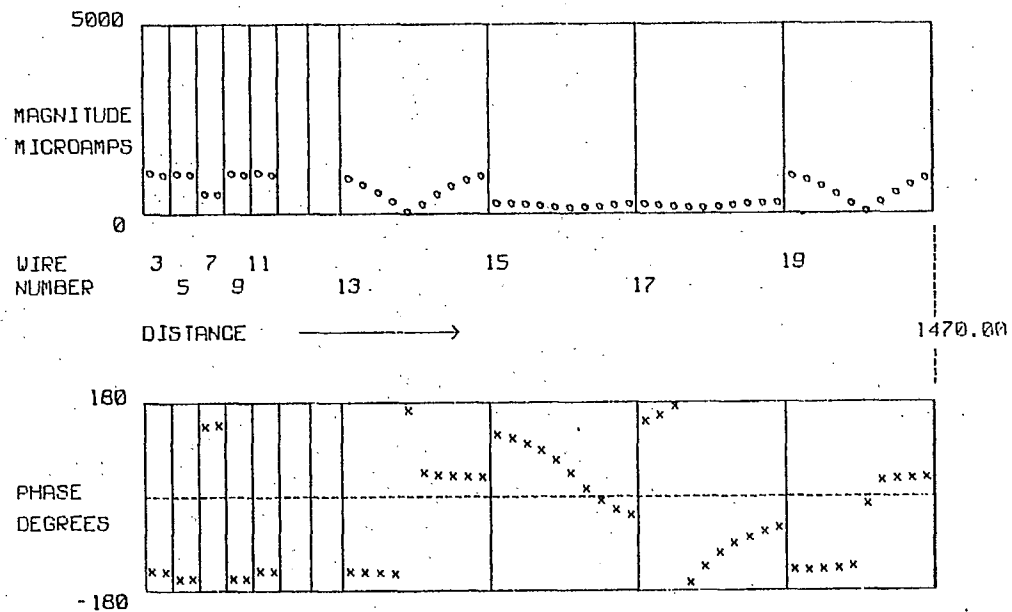


FIGURE 3.12 -

RF current distribution at 460 kHz.

WIRE RADIATOR CURRENT DISTRIBUTION

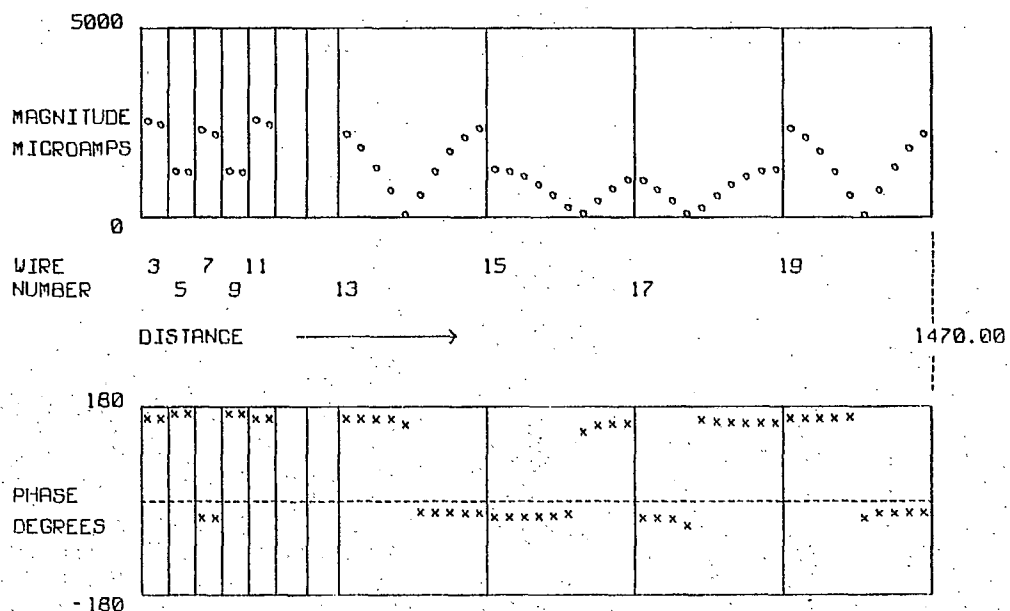


FIGURE 3.13

RF current distribution for "two wavelength double loop resonance" at 480 kHz.



FIGURE 3.14

Idealization of the RF current distribution for two wavelength double loop resonance.

WIRE RADIATOR CURRENT DISTRIBUTION

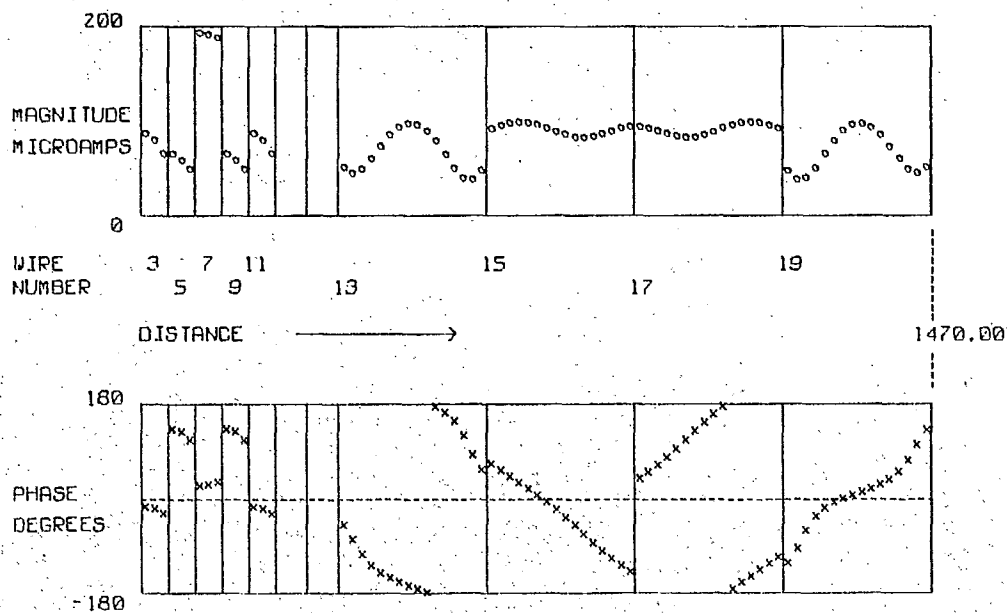


FIGURE 3.15

RF current distribution at 700 kHz.

WIRE RADIATOR CURRENT DISTRIBUTION

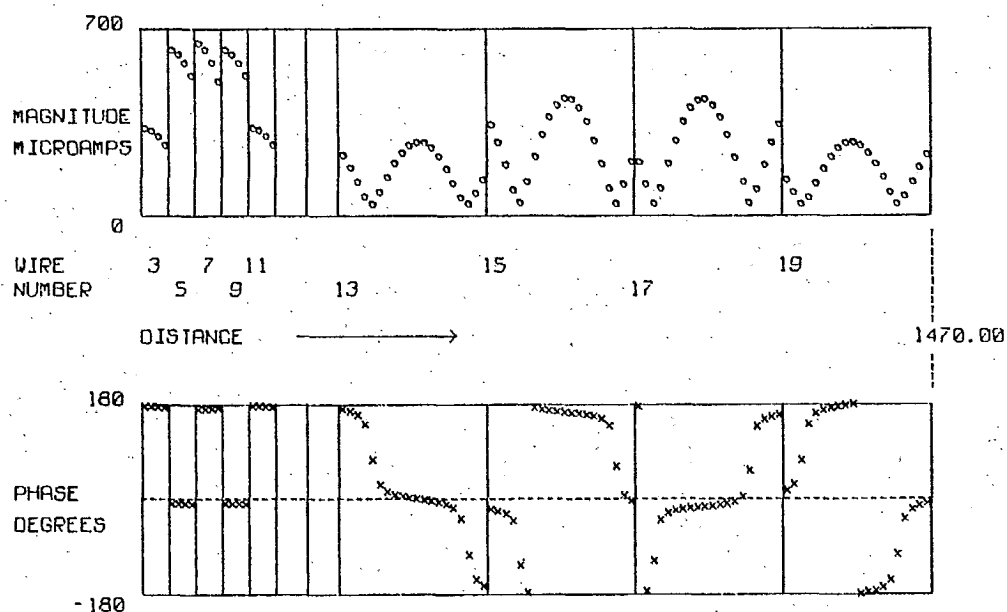


FIGURE 3.16

RF current distribution for "two wavelength loop resonance" at 840 kHz.

WIRE RADIATOR CURRENT DISTRIBUTION

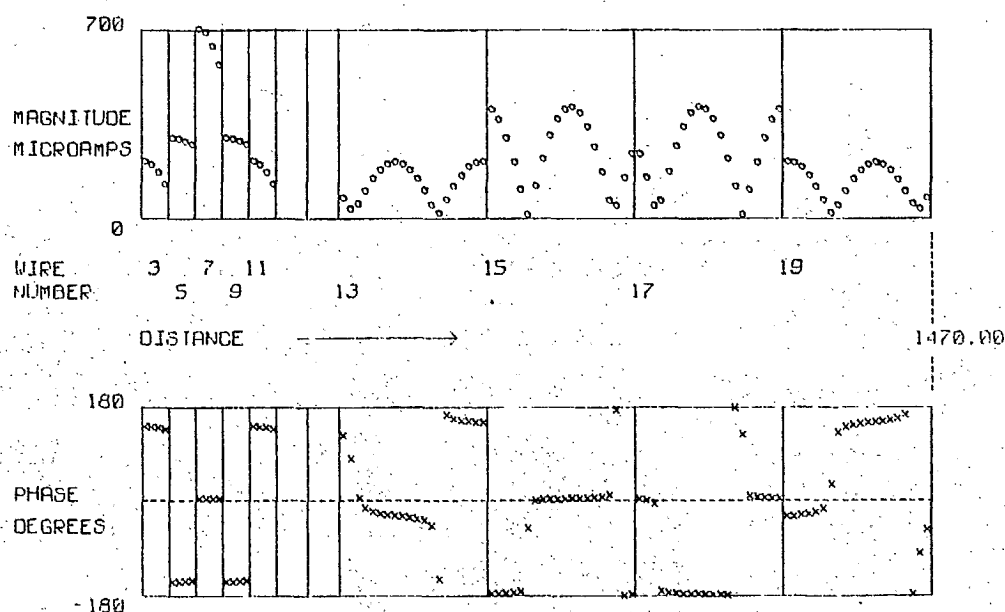


FIGURE 3.17

RF current distribution at 940 kHz for "four wavelength double loop resonance".



FIGURE 3.18

Idealization of the RF current distribution for four wavelength double loop resonance.

WIRE RADIATOR CURRENT DISTRIBUTION

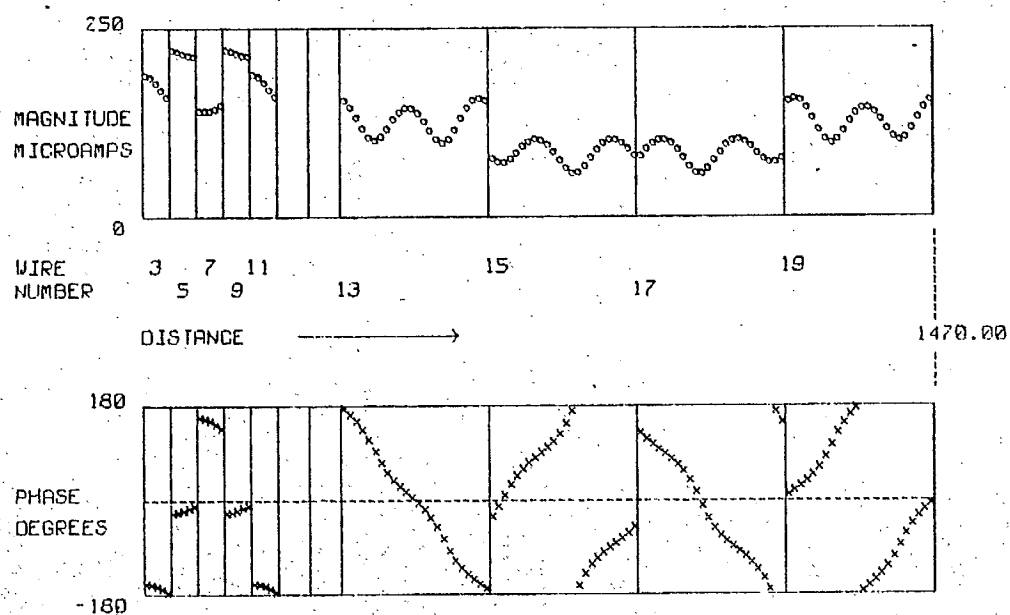


FIGURE 3.19

RF current distribution at 1100 kHz.

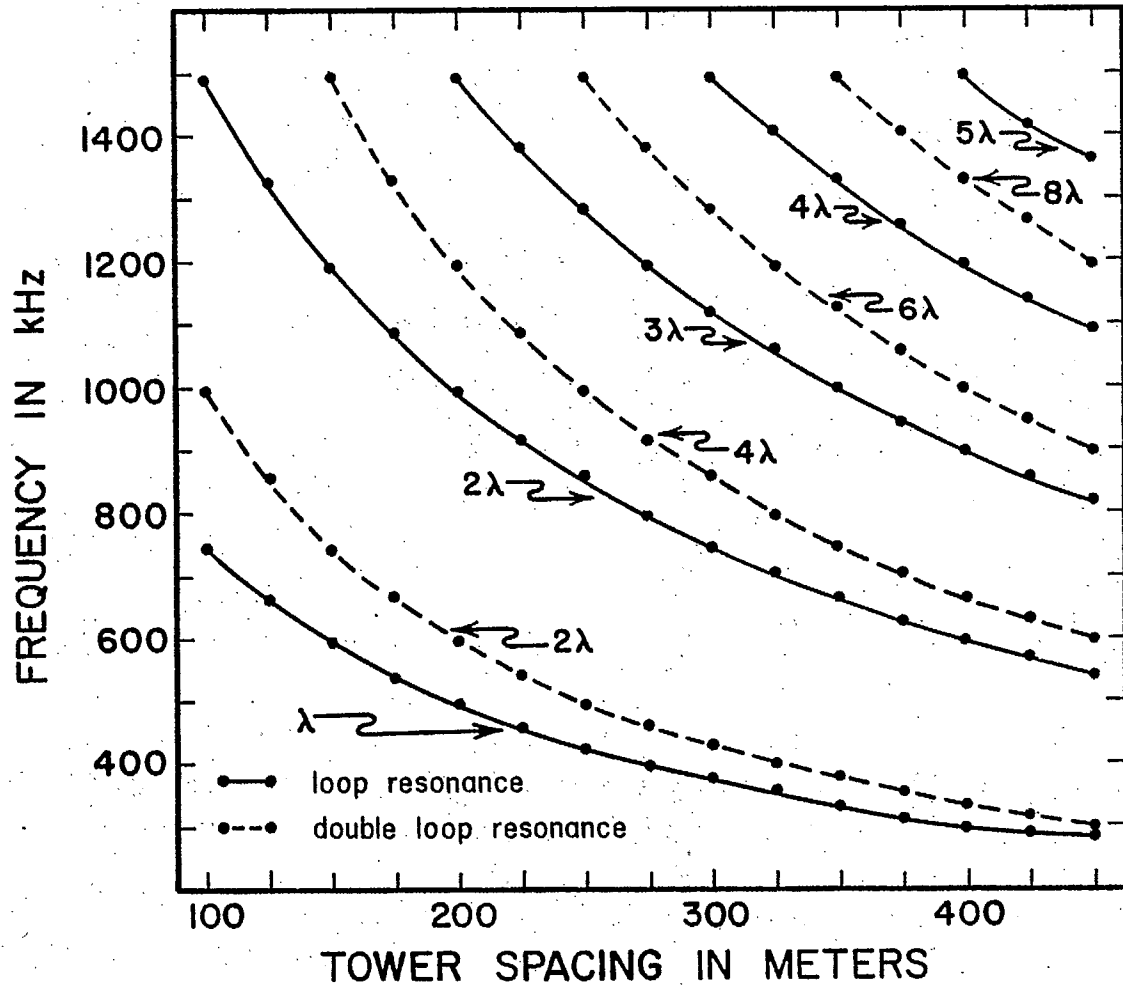


FIGURE 3.20

Resonant frequency vs. tower spacing for 50.6 m tall towers.

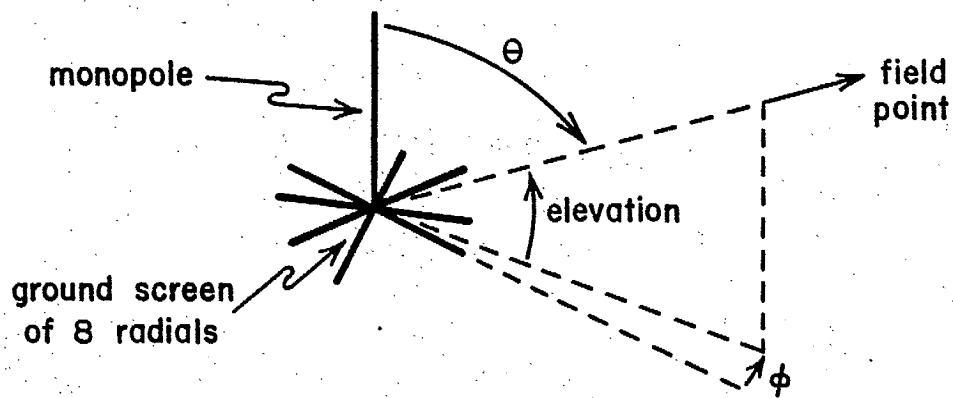


FIGURE 4.1
Monopole with eight radials.

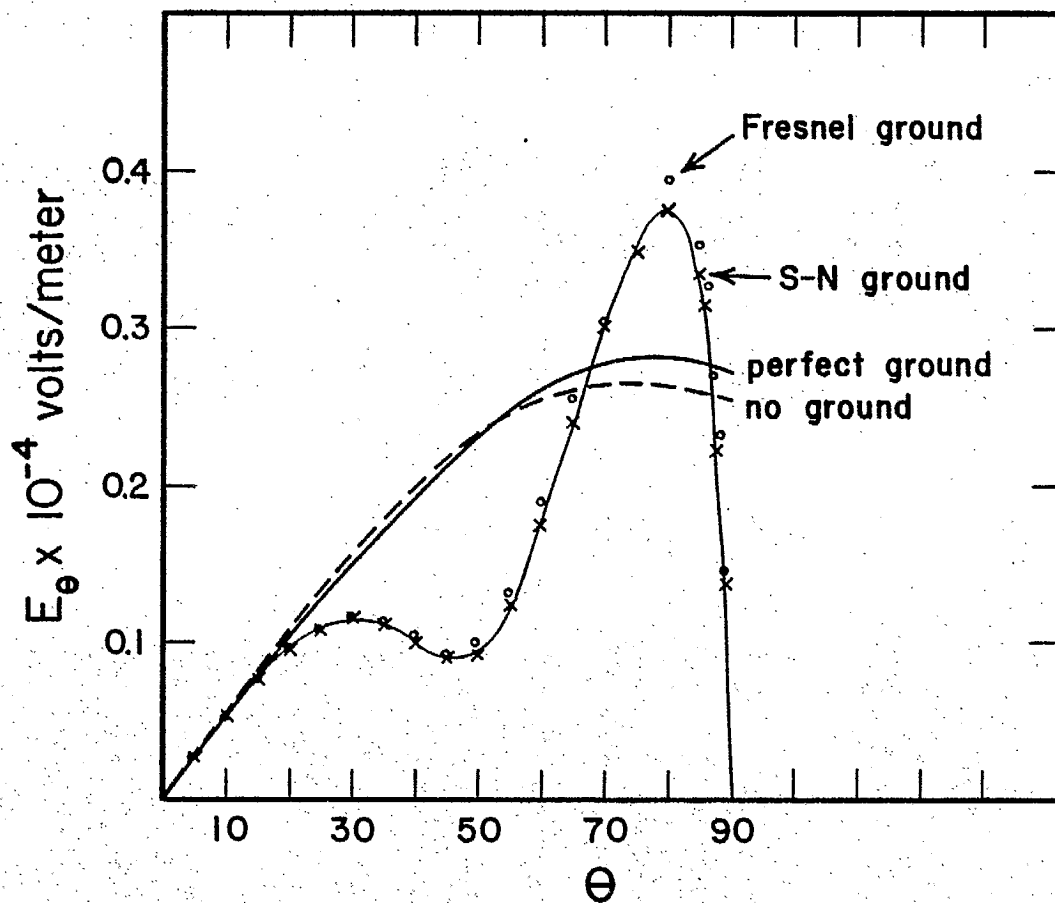


FIGURE 4.2
Elevation pattern, $\phi = 0^\circ$ at 10,000 m, antenna only

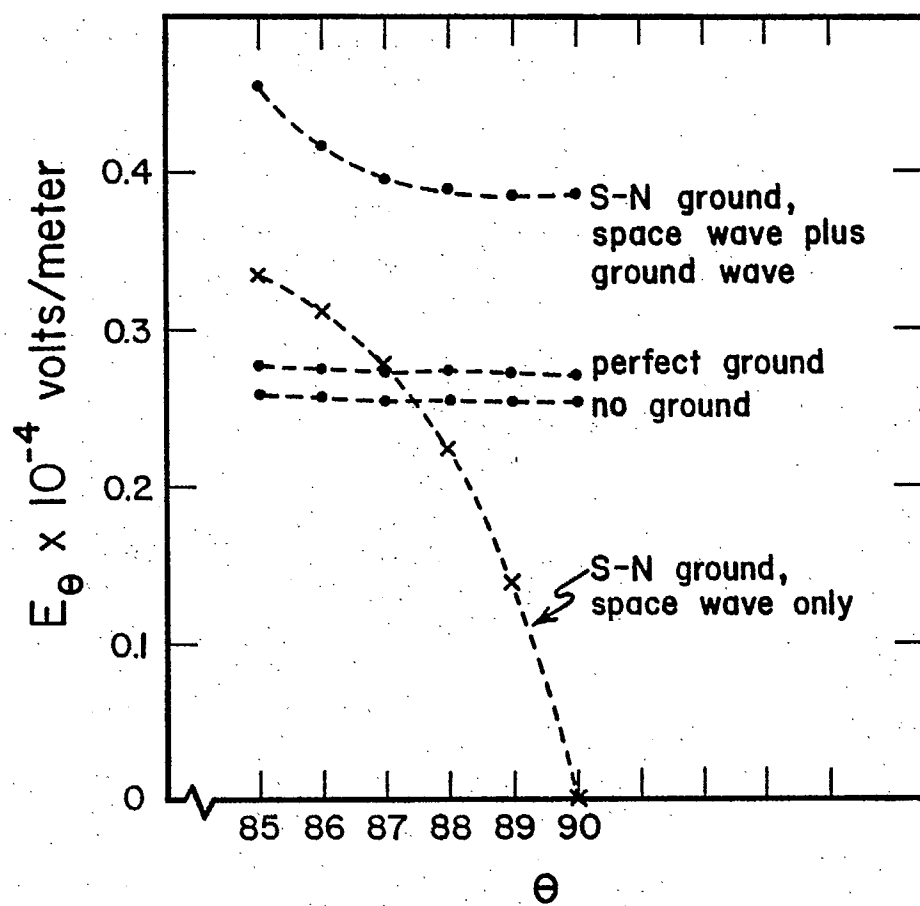


FIGURE 4.3

Detail of elevation pattern near $\theta = 90$ at 10,000 m.

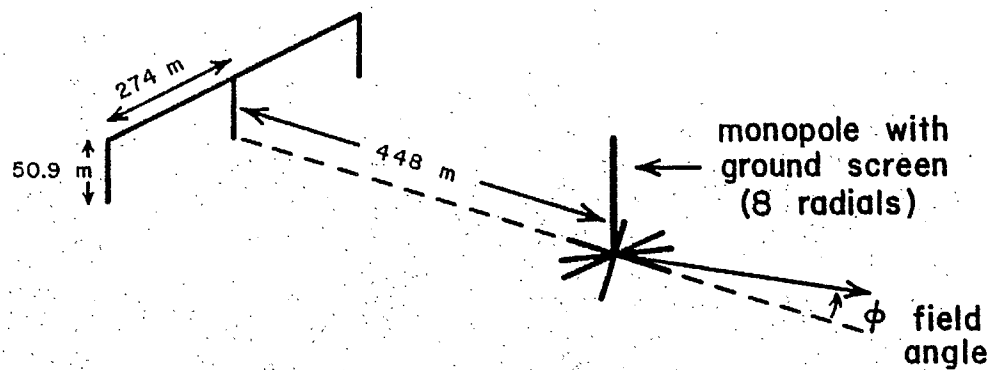


FIGURE 4.4

Antenna plus "power line".

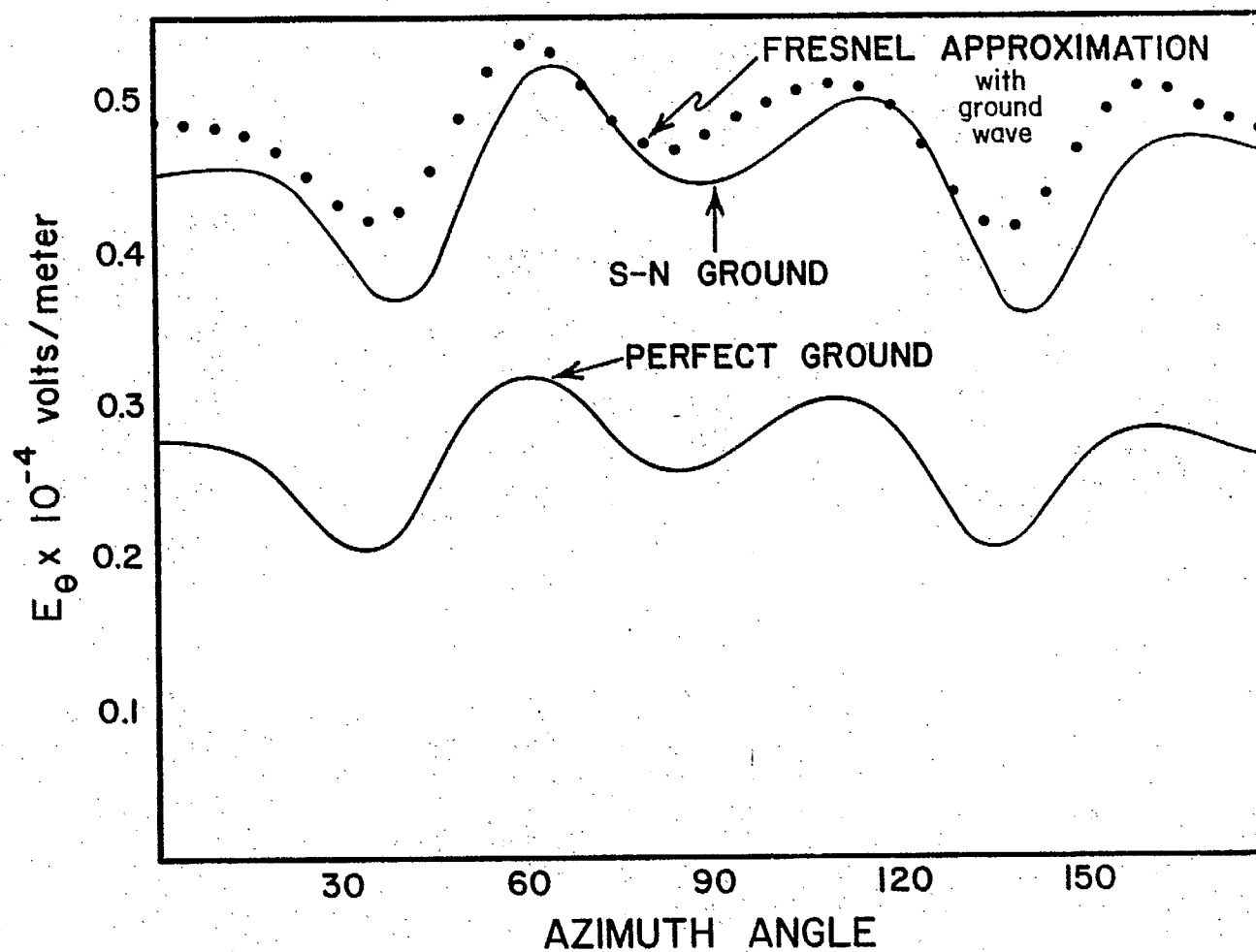


FIGURE 4.5

Azimuth pattern at 10,000 m with three ground models.

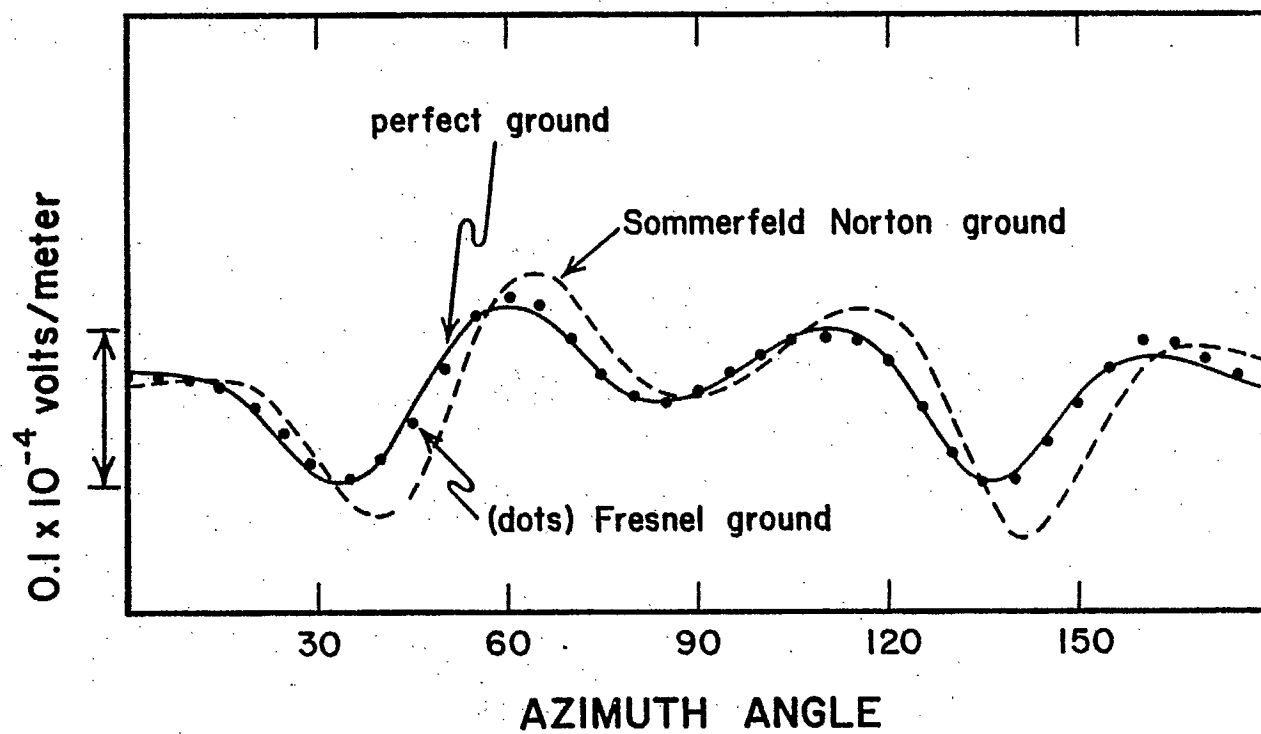
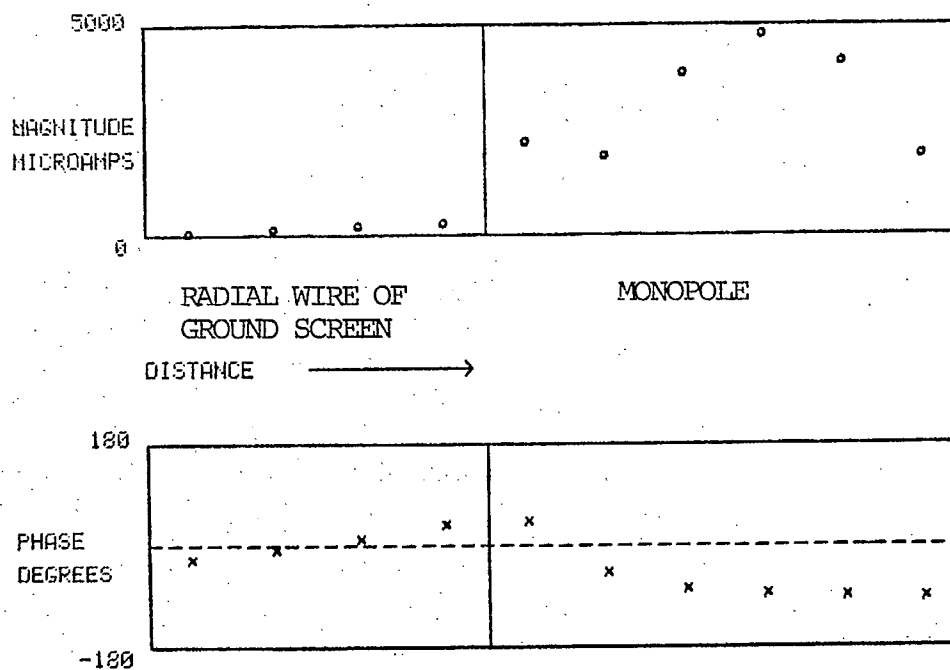
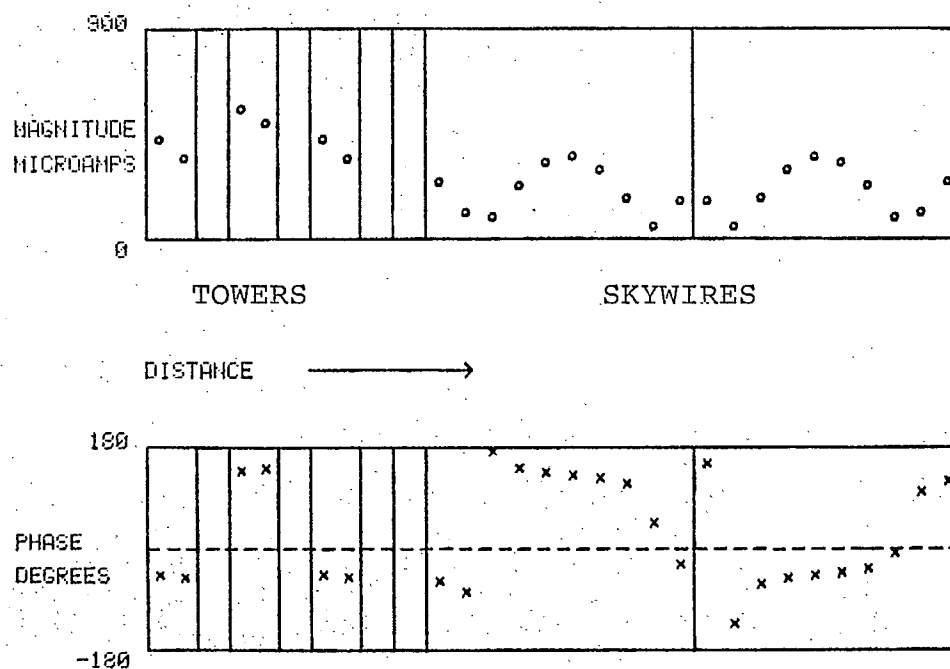


FIGURE 4.6

Comparison of the pattern with perfect ground to that with the Sommerfeld-Norton ground, and the Fresnel ground.



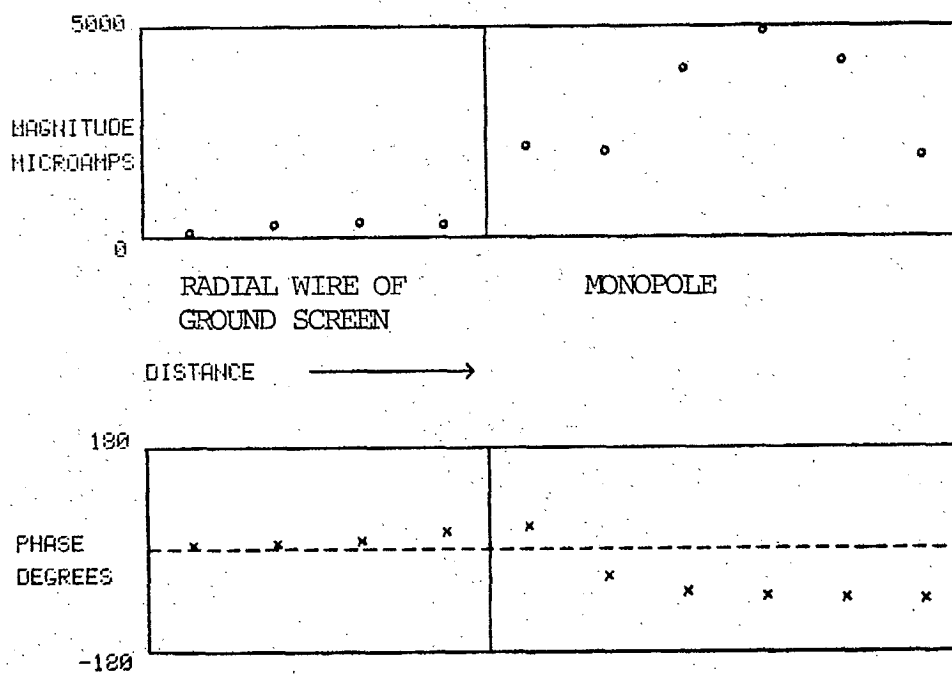
(a)



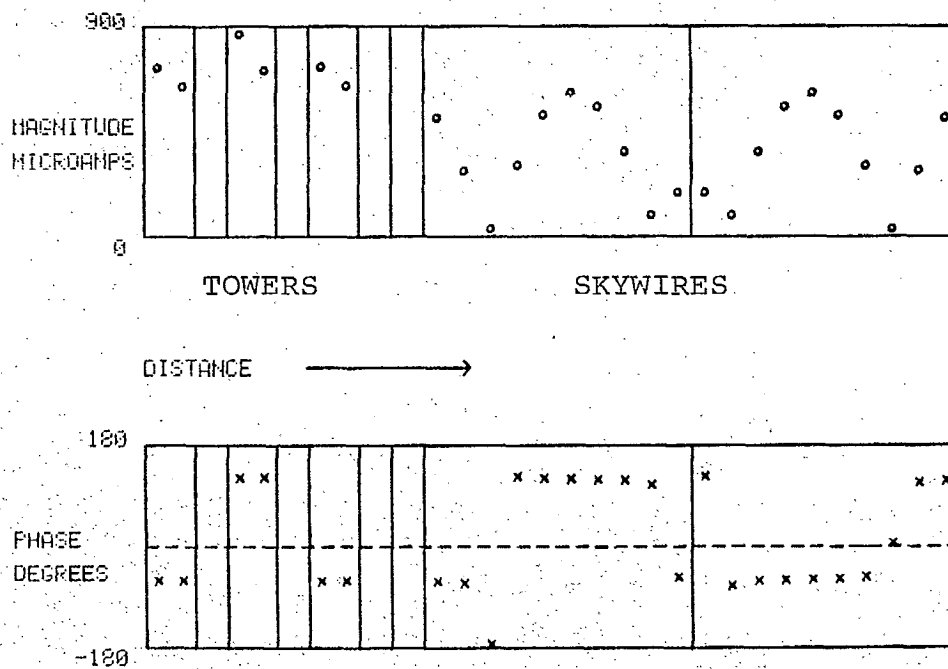
(b)

FIGURE 4.7

Current distribution with a perfect ground at 860 kHz.



(a)



(b)

FIGURE 4.8
Current distribution with the Sommerfeld-Norton ground
at 860 kHz.

--Resonant behavior and the detuning of power lines in the MF band

DUE DATE

[illegible]

CRC LIBRARY/BIBLIOTHEQUE CRC
TK6553 T787 1981 #01

INDUSTRY CANADA / INDUSTRIE CANADA



208844